

# Fgf8 and Fgf3 are required for zebrafish ear placode induction, maintenance and inner ear patterning

Sophie Léger, Michael Brand\*

Max-Planck-Institute of Molecular Cell Biology and Genetics (Dresden), Pfotenhauerstrasse 108, 01307 Dresden, Germany

Received 13 March 2002; received in revised form 9 July 2002; accepted 3 September 2002

## Abstract

The vertebrate inner ear develops from initially ‘simple’ ectodermal placode and vesicle stages into the complex three-dimensional structure which is necessary for the senses of hearing and equilibrium. Although the main morphological events in vertebrate inner ear development are known, the genetic mechanisms controlling them are scarcely understood. Previous studies have suggested that the otic placode is induced by signals from the chordamesoderm and the hindbrain, notably by fibroblast growth factors (Fgfs) and Wnt proteins. Here we study the role of Fgf8 as a *bona-fide* hindbrain-derived signal that acts in conjunction with Fgf3 during placode induction, maintenance and otic vesicle patterning. *Acerebellar* (*ace*) is a mutant in the *fgf8* gene that results in a non-functional Fgf8 product. Homozygous mutants for *acerebellar* (*ace*) have smaller ears that typically have only one otolith, abnormal semi-circular canals, and behavioral defects. Using gene expression markers for the otic placode, we find that *acelfgf8* and Fgf-signaling are required for normal otic placode formation and maintenance. Conversely, misexpression of *fgf8* or Fgf8-coated beads implanted into the vicinity of the otic placode can increase ear size and marker gene expression, although competence to respond to the induction appears restricted. Cell transplantation experiments and expression analysis suggest that Fgf8 is required in the hindbrain in the rhombomere 4–6 area to restore normal placode development in *ace* mutants, in close neighbourhood to the forming placode, but not in mesodermal tissues. Fgf3 and Fgf8 are expressed in hindbrain rhombomere 4 during the stages that are critical for placode induction. Joint inactivation of Fgf3 and Fgf8 by mutation or antisense-morpholino injection causes failure of placode formation and results in ear-less embryos, mimicking the phenotype we observe after pharmacological inhibition of Fgf-signaling. Fgf8 and Fgf3 together therefore act during induction and differentiation of the ear placode. In addition to the early requirement for Fgf signaling, the abnormal differentiation of inner ear structures and mechanosensory hair cells in *ace* mutants, pharmacological inhibition of Fgf signaling, and the expression of *fgf8* and *fgf3* in the otic vesicle demonstrate independent Fgf function(s) during later development of the otic vesicle and lateral line organ. We furthermore addressed a potential role of endomesoderm by studying *mzoep* mutant embryos that are depleted of head endomesodermal tissue, including chordamesoderm, due to a lack of Nodal-pathway signaling. In these embryos, early placode induction proceeds largely normally, but the ear placode extends abnormally to midline levels at later stages, suggesting a role for the midline in restricting placode development to dorsolateral levels. We suggest a model of zebrafish inner ear development with several discrete steps that utilize sequential Fgf signals during otic placode induction and vesicle patterning. © 2002 Elsevier Science Ireland Ltd. All rights reserved.

**Keywords:** Sensory organ; Otic placode; Otic vesicle; Inner ear; Hair cells; Lateral line; *fgf8*; *fgf3*; *Acerebellar*; Fibroblast growth factors; Induction; Zebrafish; *Danio rerio*

## 1. Introduction

The vertebrate inner ear contains the main sensory apparatus for detection of sound and gravitational stimuli. It develops from the otic vesicle or otocyst, and much of its structural complexity originates at early developmental stages. In the embryo, the otocyst forms from the otic placode, an ectodermal thickening adjacent to the hindbrain

during early somitogenesis stages (Fritzsche et al., 1998; Baker and Bronner-Fraser, 2001; Whitfield et al., 2002). Transplantation studies suggested that the placode is induced by a signal from neighbouring hindbrain (Harrison, 1935; Stone, 1931; Waddington, 1937; Woo and Fraser, 1998; Yntema, 1955), but the nature of the inducer(s) was controversial (Chisaka et al., 1992; Deol, 1964; McKay et al., 1996). Embryological and molecular evidence suggested that successive waves of inducing signals overlap in time and/or space during ear induction (Jacobson, 1966; Groves and Bronner-Fraser, 2000; Baker and Bronner-Fraser, 2001). Previous studies suggest that both the hind-

\* Corresponding author. Tel.: +49-351-210-2514; fax: +49-351-210-1359.

E-mail address: brand@mpi-cbg.de (M. Brand).

brain and the mesoderm can induce an otocyst, but that the otocyst will not differentiate unless hindbrain is adjacent to it for a critical time period (Harrison, 1935, 1945; Jacobson, 1963a, 1966; Yntema, 1950, 1955). Furthermore, no single gene is known that gives rise, when mutated, to an ear placode-less phenotype either in mouse (Steel, 1995) or in zebrafish (Malicki et al., 1996; Whitfield et al., 1996, 2002), consistent with the involvement of multiple events during placode formation.

Although the evidence is strong that a signal from hindbrain is involved in induction (reviewed in Van de Water and Represa, 1991; Torres and Giraldez, 1998; Baker and Bronner-Fraser, 2001), this signal has been difficult to find. Genetic evidence for hindbrain factors regulating otic development comes from mouse (Deol 1966; Frohman et al., 1993; Cordes and Barsh, 1994;) and zebrafish mutants (Malicki et al., 1996; Whitfield et al., 1996). Mouse mutants for *Hoxa-1*, *pax3* or *kreisler*, among others, and zebrafish mutants such as *valentino*, *mindbomb*, *snakehead*, *otter*, *fullbrain* and *spiel-ohne-grenzen* show primary defects affecting the hindbrain and associated inner ear defects (Chisaka et al., 1992; Cordes and Barsh, 1994; Dolle et al., 1993; Epstein et al., 1991; Lufkin et al., 1991; Mark et al., 1993; Moens et al., 1996, 1998; Burgess et al., 2002). The hindbrain is therefore believed to influence the development of the inner ear either directly or indirectly.

In several vertebrates, fibroblast growth factor 3 (Fgf3) is expressed in rhombomeres (rh) adjacent to the site of initial ear placode formation (Wilkinson et al., 1988; Mahmood et al., 1995; McKay et al., 1996; Lombardo et al., 1998; Phillips et al., 2001; Raible and Brand, 2001; Maroon et al., 2002). Fgfs in general function in several important cell interaction and inductive events. Fgf3 is expressed in the hindbrain and is able to induce ectopic formation of vesicles expressing some otic markers (Vendrell et al., 2000). Moreover, antisense oligonucleotide inhibition of Fgf3 caused defects in otic vesicle formation but not placode induction (Represa et al., 1991), and Fgf2 or Fgf3-coated beads can elicit formation of otic vesicles at early neural plate stages in *Xenopus* (Lombardo and Slack, 1998; Lombardo et al., 1998). Target genes for Fgf-signaling, like *sprouty2*, *erm* and *pea3*, are expressed in the otic placode during induction stages and require Fgf signaling for their expression (Chambers and Mason, 2000; Raible and Brand, 2001). However, a ‘knock-out’ of Fgf3 in the mouse causes only a mild ear phenotype, variable disruption of the endolymphatic duct (Mansour et al., 1993; McKay et al., 1994). These studies suggested that Fgf3 might be dispensable during early inner ear induction and positioning. More recent evidence implicated chick Fgf19 signaling in otic placode induction, which may signal from the paraxial mesoderm adjacent to the hindbrain or from the hindbrain primordium itself (Ladher et al., 2000), raising the possibility that Fgf3 might mimic the action of Fgf19 or other Fgfs in misexpression assays.

Morphologically, early development of the zebrafish inner ear is very similar to inner ear development of other

vertebrates (Haddon and Lewis, 1996; Fig. 1). Shortly after it becomes visible around 16 h of development, the ear placode forms the ovoid-shaped otocyst by cavitation. Within it, sensory patches with overlying otoliths form at each pole which then develops into sensory maculae containing numerous mechanosensory hair cells. Neuronal precursors delaminating from the ventral aspect of the otocyst form the statoacoustic (VIIIth) ganglion. In certain positions, the otocyst wall grows inwards forming epithelial protrusions that fuse at their tips, thus subdividing the vesicle and initiating the formation of the semicircular canals. The small islands of hair cells, or cristae, which form at the base of the semicircular canals are thought to detect angular acceleration. After about 1 week, all major components of the inner ear are present.

The optical clarity and experimental accessibility of

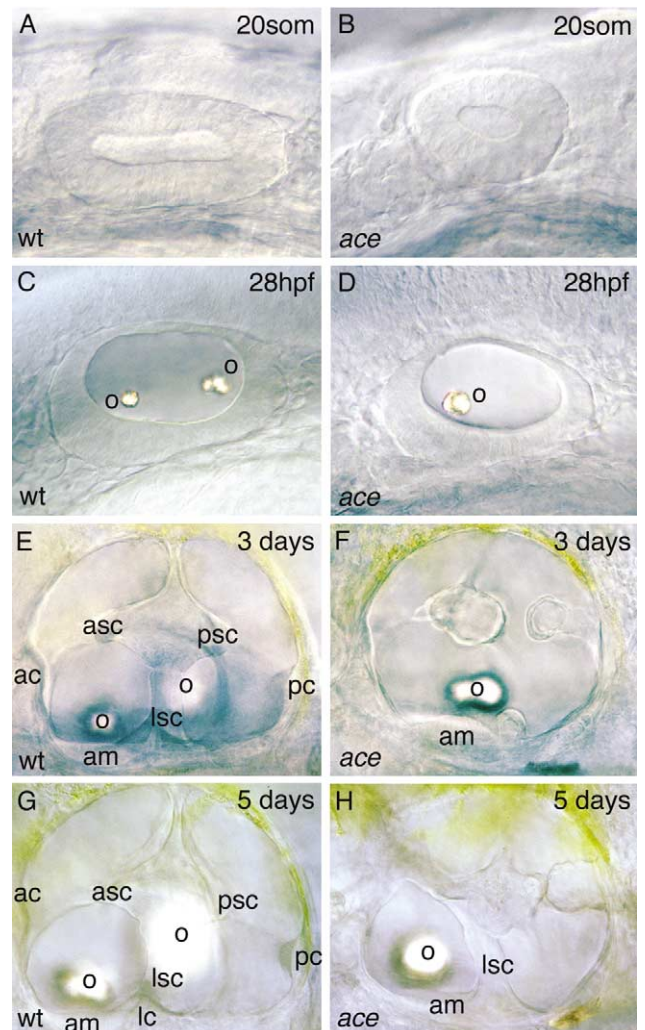


Fig. 1. Morphological development of the inner ear requires *ace/fgf8*. Lateral views (anterior to the left, dorsal to the top) of the developing inner ear in wild-type and *ace* live embryos at different developmental stages (as indicated). (o) otolith, (asc) protrusion of the anterior, (lsc) lateral, and (psc) posterior semicircular canal; (ac) anterior crista, (lc) lateral crista, (pc) posterior crista, (am) anterior macula.

zebrafish embryos has allowed the isolation of numerous mutants affecting different aspects of development or function of the inner ear (Malicki et al., 1996; Riley and Grunwald, 1996; Whitfield et al., 1996). Only a few of these mutants affect the initial formation of the otic vesicle. *Acerbellar* (*ace*) is a loss-of-function mutant in the gene encoding the Fgf8 signaling protein, and affects morphology of the inner ear (Brand et al., 1996; Reifers et al., 1998). Here we study the activity and function of Ace/Fgf8 and Fgf3 in detail, and of Fgf signaling more generally, in development of the inner ear. Our work partially confirms and extends the results of two other independent studies (Phillips et al., 2001; Maroon et al., 2002). Similar to these studies, we find that pharmacological inhibition and morpholino-antisense-induced knock-down (Nasevicius and Ekker, 2000) of *fgf3* and *fgf8* in wild-type and *ace* mutant backgrounds reveals that Fgf3 and Fgf8 are redundantly required for early ear placode formation. We furthermore find that this requirement includes onset of *pax8* expression as the earliest known marker of otic development, as well as other markers. In addition, we provide evidence from cell transplantation studies showing that Fgf8 is required in the hindbrain including rhombomere 4, a site of *fgf8* and *fgf3* expression, in close neighbourhood to the forming placode. Consistent with the results of our transplantation experiments, and differing from the results obtained by Phillips et al. (2001), we find that placode induction can proceed largely normally in the absence of cephalic endomesoderm in embryos lacking Nodal-signaling. We also find that Fgf8 is sufficient for normal induction of the ear placode in a subset of the ectoderm, and that Fgf's function independently of early induction again during later stages in patterning the otic vesicle. We suggest that Fgf8 and Fgf3 are *bona-fide* hindbrain-derived inducers of inner ear development and differentiation that induce otic placode formation and control patterning of the otic vesicle at later stages.

## 2. Results

### 2.1. Morphological development in the inner ear requires *ace/fgf8*

In wild-type embryos, the otic placode becomes first visible around 16 h of development as a thickening of the ectoderm which then cavitates to generate the otic vesicle containing two otoliths in stereotype locations at the opposite end of the vesicle (Figs. 1A,C). Ear development in homozygous *ace* mutants (*ace*<sup>-</sup>) is morphologically abnormal from the beginning, since the size of the otic placode and vesicle is variably reduced to about half the wild-type size (Fig. 1B; Brand et al., 1996). At 28 h, 50% of *ace*<sup>-</sup> ears (*n* = 157) have only one otolith, and even if both are present, they are typically misplaced and very close to or even touching each other (Figs. 1D,F). In 24% of the mutants, the single otoliths are of abnormal shape, suggest-

ing that they might result from the fusion of the otoliths (see below). The epithelial protrusions subdividing the vesicle into semicircular canals (scc) are abnormal in 40% of *ace*<sup>-</sup> ears (*n* = 120); they usually arise in abnormal positions and some protrusions are missing. The protrusions often fail to elongate and fuse (Figs. 1E–H). However, ears with only one otolith can develop a relatively normal scc system and vice versa, suggesting independent functions for Ace/Fgf8 in different parts of the inner ear. Towards later stages of development, *ace*<sup>-</sup> ears become increasingly normal compared to the wild-type, although the morphological defects always remain apparent (see Figs. 1G,H, and below).

### 2.2. Abnormal behavior of *ace/fgf8* mutants

Abnormalities of the vestibular system are often linked to abnormal motor behavior, and indeed the morphological defects of *ace*<sup>-</sup> larvae are associated with abnormal behavior. On day 5 of development, wild-type larvae have straight tails, inflated swim bladders, and swim dorsal side up. Sibling mutant larvae typically have a slightly undulated tail and swim or lie on their sides. In addition, *ace*<sup>-</sup> larvae react abnormally to tactile stimuli: wild-type embryos, upon touching the head or tail with a blunt glass capillary, move straight for at least one full body length, or dash off altogether. In contrast, 80% of the *ace*<sup>-</sup> larvae (*n* = 54) do not escape but rather circle on the spot. Such circling behavior often reflects a dysfunction of the vestibular system (Nicolson et al., 1998). In addition, *ace*<sup>-</sup> larvae appear less sensitive to stimulation on the head than on the tail, whereas wild-type larvae react to both stimuli with a similar escape response. In response to a vibrational stimulus (gentle tapping on the rim of the petri dish) *ace*<sup>-</sup> larvae hardly react: 80% (*n* = 48) fail to swim away from the position of the vibrational stimulus as wild-type larvae normally do. A total of 38% of *ace*<sup>-</sup> embryos (*n* = 48) respond only by half a turn, and 43% (*n* = 48) do not move at all. Given the absence of the cerebellum and abnormal brain development in *ace*<sup>-</sup>, these behavioral defects probably have multiple origins, but we note that they are also consistent with the defects in the auditory-vestibular and lateral line system described below.

### 2.3. *fgf8* expression in the otic vesicle

We examined *fgf8* expression by in situ hybridization (ISH) during ear development, and compared it to expression in *ace*<sup>-</sup> ears. Importantly, *fgf8* is initially not expressed in the forming placode itself (see Section 2.4). In the otic vesicle, expression is first observed from 18 h of development onwards. *fgf8* is expressed in an anterior patch from which the anterior macula will develop and more weakly and transiently, at the posterior-medial pole (Figs. 2A,B). Anterior expression is initially normal in *ace*<sup>-</sup> compared to wild-type otic vesicles. Posterior expression is extinguished in wild type vesicles at 24 h, but remains detectable in some

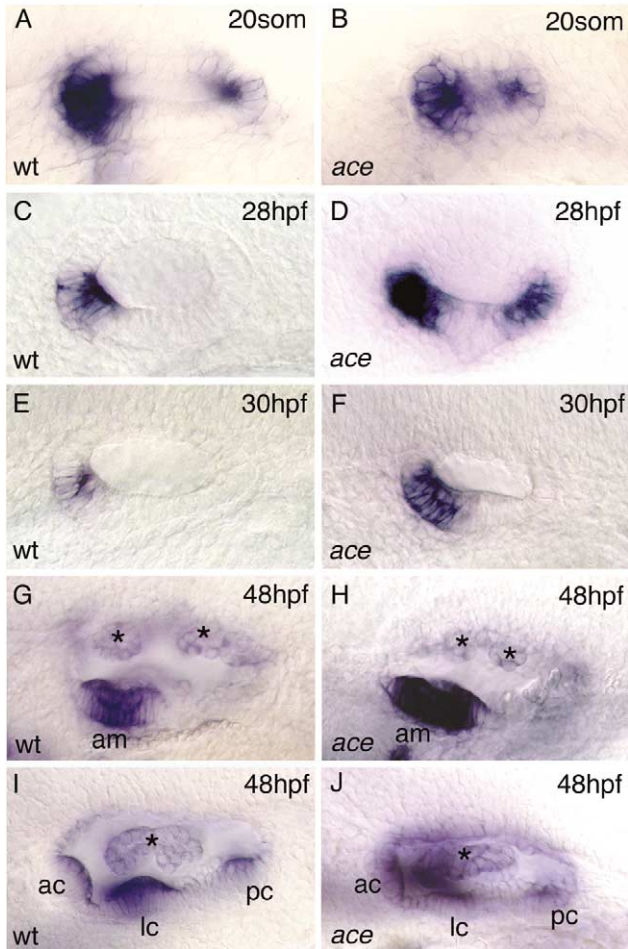


Fig. 2. *fgf8* expression in the otic vesicle. Lateral views of wild-type and *ace*<sup>-</sup> otic vesicles at different developmental stages (as indicated). (am) anterior macula, (ac) anterior crista, (lc) lateral crista, (pc) posterior crista, (\*) protrusions of the semicircular canals.

*ace*<sup>-</sup> vesicles until 28 h (Fig. 2D), giving the vesicle a more symmetric appearance in the mutants. Persistence of posterior pole expression may be due to a general failure in feedback regulation in *ace*<sup>-</sup> mutants (Reifers et al., 1998; Shanmugalingam et al., 2000; Fürthauer et al., 2001). At 30 and 48 h of development, *fgf8* upregulation is also visible in an apparently increased number of cells in the anterior patch (Figs. 2E–H). From 48 h onwards, *fgf8* is expressed somewhat more strongly in the luminal cell layer of the anterior macula containing the hair cells, and in the cristae and the epithelial protrusions of the scc system (Figs. 2G–J). The dynamic and spatially ordered expression of *fgf8* and the defects observed in *ace*<sup>-</sup> suggests that *fgf8* might function during several distinct steps of otic vesicle differentiation.

#### 2.4. Induction of the otic placode requires *ace*/*Fgf8*

On a gastrula-stage fate map, the otic primordium arises adjacent to the anterior hindbrain (Kozlowski et al., 1997),

and although *fgf8* is not expressed in the forming placode itself, it is expressed during gastrulation and early somitogenesis in close proximity to it. From 70% epiboly onwards, *fgf8* is initially expressed throughout the anterior hindbrain and becomes then restricted during early somitogenesis to rhombomere 4 (r4), ventral r2, r1 and the midbrain-hindbrain-boundary (MHB) (Fürthauer et al., 1997; Reifers et al., 1998). In addition, *fgf8* is expressed in the mesodermal heart field underlying the ectoderm just anterior to the site of ear placode formation (Reifers et al., 2000a). Because *fgf8* is not expressed in the otic placode prior to the 18 somite stage, and because placode size is reduced in *ace*<sup>-</sup> embryos, this suggested that *fgf8* could induce placode formation from surrounding tissue. We therefore studied marker gene expression by ISH that reveal the early events of placode formation prior to morphological differentiation

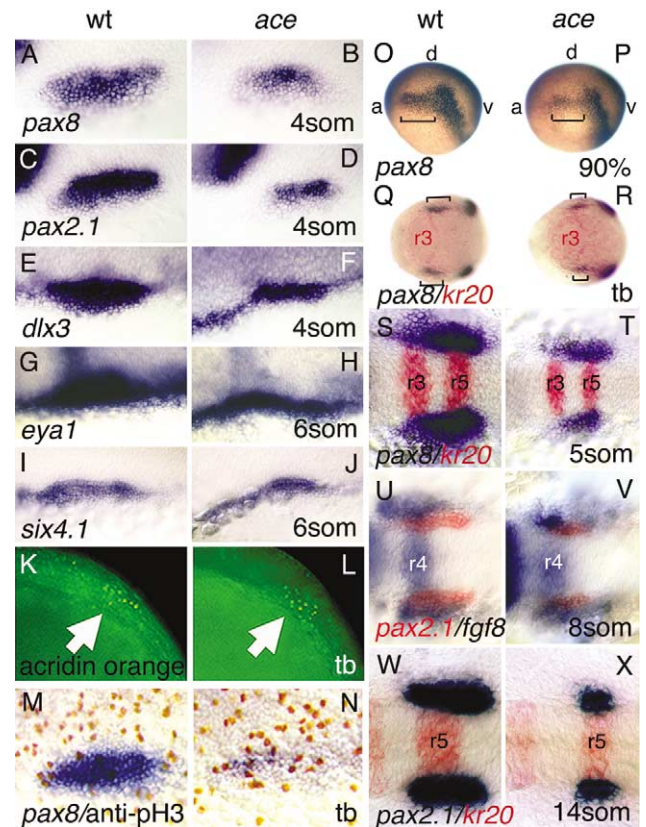


Fig. 3. Induction of the otic placode marker gene expression requires *ace*/*fgf8*. (A–J) Expression of early otic markers in the otic primordium (bracket) of wild-type and *ace* embryos (markers as indicated). Dorsal views, anterior to the left, except for K, L and O, P (lateral views). (K, L) Acridine orange staining does not detect increased numbers of dying cells in the otic primordium (arrow) of *ace* mutants. (M, N) Staining with an anti-phosphohistone antibody recognizing mitotic cells (in brown) and ISH to *pax8* to visualize the otic primordium; a similar number of mitotic cells is apparent. (O–R) Expression of *pax8* in the wild type and in the *ace*<sup>-</sup> otic primordium (bracket) at the indicated stages. (a) animal pole, (v) vegetal pole, (d) dorsal side. (Q–X) Position of the otic placode relative to rhombomeres forming in the hindbrain; double ISH with a placode marker (*pax8* or *pax2.1*, as indicated) and a rhombomere marker (*Krox20* or *fgf8*, as indicated). (r3), (r4) and (r5), rhombomeres 3, 4 and 5, respectively.

(Fig. 3) and performed RNA injections, Fgf8-bead implantations (Fig. 6), cell transplantations (Fig. 7), pharmacological inhibition of Fgf-signaling (Fig. 9) and morpholino-inactivation of *fgf8* (Fig. 10); together, these studies provide evidence that Fgf8 acts as a placode inducer acting from the hindbrain primordium.

*pax2.1* (Krauss et al., 1991), *dlx3* (Ekker et al., 1992), *pax8* (Pfeffer et al., 1998), *eyal* (Sahly et al., 1999) and *six4.1* (Kobayashi, 2000) are among the first genes to be specifically activated or upregulated in the otic primordium from late gastrulation stages onwards. The otic placode forms from the primordium by thickening within the *dlx3*, *eyal* and *six4.1*-expressing stripe bordering on the neural plate (Akimenko et al., 1994; Sahly et al., 1999; Kobayashi, 2000). In *ace* mutants, the stripe is unaffected, but expression of all these markers in the placode arising from it occurs in a smaller territory that is at most half the size of the wild-type placode (Figs. 3A–J). *pax8* may be the earliest marker for ear placode formation (Pfeffer et al., 1998), and is expressed in the otic primordium from 85 to 90% epiboly onwards. *pax8* expression is initially located adjacent to much or all of the hindbrain primordium, roughly corresponding to fate map position of the inner ear placode. Subsequently, starting at 95% epiboly, *pax8* expression becomes progressively restricted to the placodal area (Figs. 3O–R). Double-ISHs with *pax2.1*, *fgf8*, *pax8* and *krox20* probes (Figs. 3Q–X) show that otic placode development, as monitored by *pax8* expression, is initiated immediately adjacent to the *fgf8*-expressing cells in the hindbrain primordium of both wild-type and *ace*<sup>-</sup> embryos, covering an area approximately adjacent to r2–6 (Figs. 3Q–T). Within the domain of *pax8* and *pax2.1* positive cells, higher levels of expression then develop next to r4 and r5 (Figs. 3S–V), and by the 8-somite stage, expression of *pax2.1* is concentrated next to r4 and r5 (Figs. 3U, V). Thus, during gastrulation stages, placodal development starts next to most of the hindbrain posterior to r2, and then becomes progressively restricted during early somitogenesis stages to an area next to r4–6, and thus closely follows *fgf8* expression during these stages. During later somitogenesis stages, the placode is located predominately next to r5 and r6 (Figs. 3W, X), perhaps due to an anterior shift of the hindbrain that has been described previously (Moens et al., 1996). In *ace*<sup>-</sup> mutants, placodal marker expression is initially reduced throughout, then becomes reduced to about half the normal size transiently next to r4, and expression then persists next to r5 (Figs. 3W, X). *pax8* expression is already slightly reduced in the otic primordium of *ace* mutants at its onset during late epiboly stages, and more strongly so from tailbud stage onwards (Figs. 3O–T).

Because Fgf8 might act as a survival factor or mitogen on placodal cells, marker gene expression might be indirectly reduced in *ace* mutants through cell death or altered proliferation of placodal cells. We therefore examined *ace*<sup>-</sup> embryos using acridine orange to detect dying cells between 70% of epiboly and the 6-somite stage, and with an anti-

phospho-histone antibody recognizing mitotic cells at tailbud, 5, 10 and 20 somite-stage, and at 24 h, and find no difference to wild-type embryos. Although difficult to quantify, the amount of dying and of mitotic cells in the otic primordium of *ace* mutants appears similar to that in wild-type siblings (Figs. 3K–N). Once the placode is formed, its cells appear to be of normal size in the mutants (not shown). Together with the gene expression data, this suggests that the defect in *ace* mutants is due to a failure in otic placode induction.

### 2.5. Requirement for *ace/fgf8* during otic vesicle differentiation and neurogenesis

The morphological defects of *ace*<sup>-</sup> otic vesicles and the *fgf8* expression pattern suggested that *fgf8*, in addition to its function during placode induction, might also function during otic vesicle differentiation. Different parts of the otic vesicle at 20–24 h of development are altered in *ace*<sup>-</sup> embryos. *pax5* expression marks an anterior-medial domain of the otic vesicle, which is reduced in *ace*<sup>-</sup>, as is *mshD* expression in the dorsal vesicle (Figs. 4A, B, E, F; Ekker et al., 1992). *otx1* (Li et al., 1994), *gsc* (Thisse et al., 1994) and *zdk1* (not shown) mark a ventromedial or posterior domains that are almost eliminated in *ace* mutants (Figs. 4I, J, M, N).

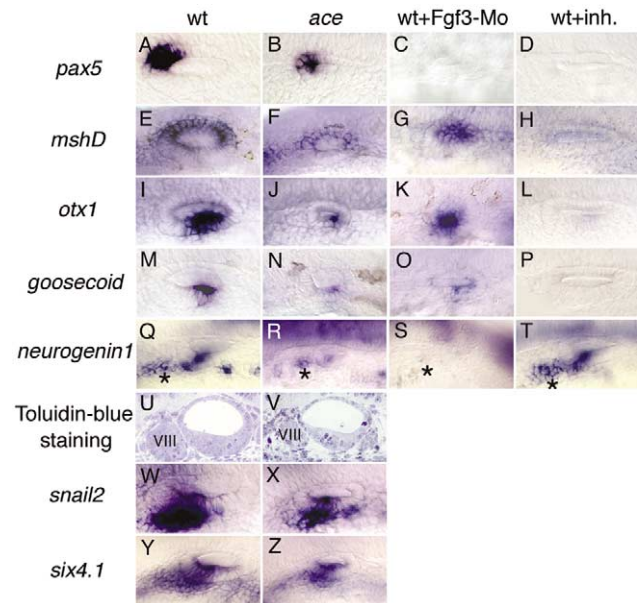


Fig. 4. Requirement of Fgf8 and Fgf3 during otic vesicle differentiation and neurogenesis. (A–P) Expression of marker genes for different parts of the otic vesicle at 24 hpf in wild-type and *ace* embryos and wild type embryos injected with Mo-*fgf3* or treated with the SU5402 inhibitor from the 18-somite stage to 24 hpf, as indicated. Dorsal views except for (E–H), lateral views (anterior to the left). (U, V) Toluidin-blue stained parasagittal section of a wild-type (U) and an *ace* (V) embryo at 36hpf, taken at the level of the eighth ganglion (VIII). (Q–T, W–Z) Expression of neurogenic markers (as indicated) in the vesicle and in the eighth ganglion (\*) at 24 hpf in wild-type and *ace* embryos and wild type embryos injected with Mo-*fgf3* or treated with the SU5402 inhibitor from the 18-somite stage to 24 hpf, as indicated. Lateral views (anterior to the left).

Thus, in spite of the reduced vesicle size, many aspects of differentiation proceed normally in *ace*<sup>-</sup> vesicles on a reduced scale; ventromedial (*otx1*-positive) and posterior vesicle development may be somewhat more strongly affected than other vesicle parts.

Neurons of the stato-acoustic (VIIIth) ganglion innervating the hair cells, detected by time-lapsing or using a *pax2.1*-GFP transgenic line, delaminate from the ventral wall of the otic vesicle mainly between 22 and 42 h of development, where they collect underneath the otic epithelium (Haddon and Lewis, 1996; Picker et al., 2002). Development of the eighth ganglion is affected in *ace*<sup>-</sup> mutants. In parasagittal sections of 36 h wild-type and *ace* embryos, *ace*<sup>-</sup> otic vesicles are reduced in size and the eighth ganglion is much smaller than in wild-type vesicles (Fig. 4Q,R). *neurogenin1* is a marker for early neuronal development (Korzh et al., 1998). In wild-type embryos *neurogenin1* is expressed in the ventral vesicle wall, the forming VIIIth ganglion, and in unidentified cells posterior to it; expression in the VIIIth ganglion is strongly reduced in *ace*<sup>-</sup> embryos, apparently labelling fewer cells (Figs. 4Q,R). Other markers of early neurogenesis of the eighth ganglion are similarly reduced, like *snail2* (Thisse et al., 1995), *six4.1* and *nkx5.1* (Figs. 4W–Z; Adamska et al., 2000). We suggest that the reduced ventral portion of the *ace*<sup>-</sup> otic vesicle secondarily leads to the smaller size of the eighth ganglion, due to a smaller domain in which neurogenesis can occur.

## 2.6. Hair cell organization is affected in *ace*<sup>-</sup>/*fgf8* mutants

The behavioral defects, abnormal otolith formation and the *fgf8* expression suggested a possible role for Ace/Fgf8 in the development of mechanosensory hair cells. *msxC* is a homeobox gene marking the developing cristae epithelium (Ekker et al., 1992), and *msxC* expression in particular of the lateral crista is strongly reduced in *ace*<sup>-</sup> ears (Figs. 5A,B). We also observed reduction of *pax5* expression in the anterior macula, and of *zdk1* expression in the posterior macula of *ace*<sup>-</sup> ears at 24 and 48 h (Figs. 4A,B and data not shown). To analyze hair cell development in *ace*<sup>-</sup> mutants, we stained the actin-rich stereocilia of the hair cells with fluorescent phalloidin (FITC-phalloidin) on day 5, and analyzed them by confocal microscopy. In *ace*<sup>-</sup> mutants the sensory patches of the ear are misplaced, especially the three cristae, probably reflecting the distorted morphology of the vesicle (Figs. 5E–G). Also, the number of hair cells in *ace*<sup>-</sup> ears is variable, but always reduced: on day 5, the wild-type anterior macula contains on average  $75 \pm 3$  ( $n = 2$ ) hair cells, whereas *ace*<sup>-</sup> ears contain  $55 \pm 12$  ( $n = 8$ ). Typically, *ace*<sup>-</sup> ears with fewer hair cells also have only one otolith that is always either anterior or medial, but never posterior in position. Fig. 5G shows the strongest *ace* phenotype we observed: this ear has only one otolith, and the number of hair cells of the lateral and posterior cristae is strongly reduced. Moreover, there is only one macula with about 40 hair cells which is located in the medial part of the

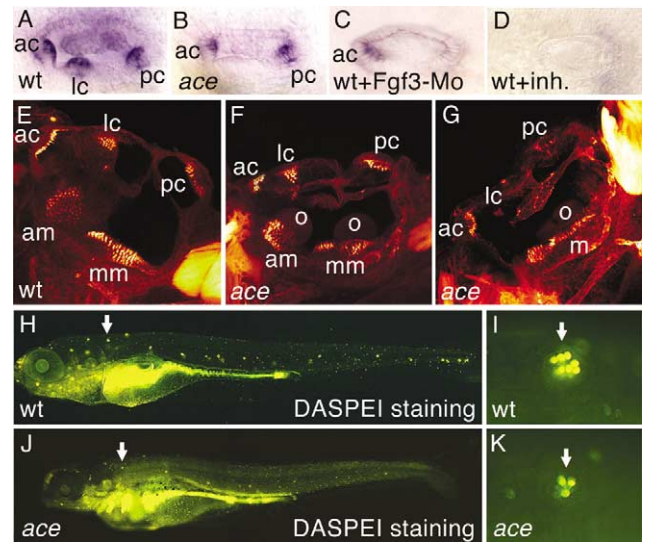


Fig. 5. Hair cell organization is affected in *ace/fgf8* mutants. (A–D) Expression of *msxC* in the developing cristae at 48 hpf in wild-type (A) and *ace* (B, C) embryos and in wild type embryos injected with Mo-*fgf3* (C) or treated with the SU5402 inhibitor from 24 to 48 hpf (D). Lateral views. (E–G) Fluorescent phalloidin staining of the actin-rich stereocilia of the hair cells at day 5 of development in wild-type (E) and *ace*<sup>-</sup> (F, G) inner ears. Lateral views obtained by projection of several optical sections to show all the hair bundles of the hair cells. Each hair bundle corresponds to one hair cell. (F) weak *ace*<sup>-</sup> phenotypes. (G) strongest *ace*<sup>-</sup> phenotype found; see text. (ac) anterior crista, (lc) lateral crista, (pc) posterior crista, (am) anterior macula, (mm) medial macula, (m) macula, (\*) epithelial protrusions of the semi-circular canals, (o) otolith. (H–K) DASPEI staining of the hair cells of the lateral line neuromasts at day 5 of development in wild type (H, I) and *ace*<sup>-</sup> (J, K) embryos. (I, K) closer view of the neuromast indicated by an arrow in (H) and (J), respectively.

otocyst, but spreads more anteriorly than the normal medial macula, probably reflecting a fusion of the anterior and the medial macula. The single otolith appears composed of two parts, which may reflect a partial fusion, since otoliths form owing to and in association with the maculae (Riley et al., 1997). In conclusion, positioning of the sensory patches, hair cell number and otolith development are variably abnormal in *ace*<sup>-</sup> mutants, probably reflecting a mixture of direct and indirect effects of the lack of *fgf8* on otic vesicle and sensory hair cell differentiation.

Placodally-derived mechanosensory hair cells similar to those of the inner ear also occur in the neuromasts of the lateral line, suggesting that they may share common developmental programs indicative of a common evolutionary ancestry (Northcutt, 1986; Jorgensen, 1989; Platt et al., 1989). We therefore asked if *ace*<sup>-</sup> larvae have normal neuromasts by staining the neuromast hair cells with the fluorescent dye DASPEI (Whitfield et al., 1996) and counting neuromasts on both sides of the body. Compared to wild-type larvae ( $25 \pm 0$  neuromasts,  $n = 10$  sides), *ace*<sup>-</sup> larvae have strongly reduced numbers of neuromasts ( $9.7 \pm 5$  neuromasts per side,  $n = 30$  sides); head neuromasts appear somewhat less strongly reduced (Figs. 5H,J). In addition, the number of hair cells per neuromast is vari-

able, but reduced overall; a representative case is shown in Figs. 5I,K. To determine if lateral line placode formation is occurring normally, we examined *eya1*, *six4.1* and *nkx5.1* as markers of the lateral line placode, but expression was unaffected at 24 h in *ace*<sup>-</sup> embryos, and the placode was in a similar position along the anterior-posterior axis as in the wild type siblings (not shown; *eya1* is also normal at 48 h). Thus, lateral line placode formation and migration apparently proceeds normally in *ace*<sup>-</sup> mutants, but a later, as yet unknown step of neuromast development requires *fgf8* function. Consistent with this possibility, the lateral line placode and migrating primordium expresses the Fgf target gene *pea3* and Fgf-R1 (Münchberg et al., 1999; Raible and Brand, 2001; C. Thisse and B. Thisse, personal communication).

### 2.7. *Fgf8* can expand ear placode territory

Abnormal ear development of *ace*<sup>-</sup> mutants clearly has an early origin during placodal induction stages, and we therefore focussed on understanding the role of *fgf8* during the initial, inductive step. Our above analysis indicated that *fgf8* is required for induction of a normal sized placode. In order to test whether *fgf8* is also sufficient to specify placodal fate, we injected *fgf8* mRNA into one side of the embryo, or we implanted Fgf8 protein coated beads prior to placode formation (Figs. 6A,D). Control injections with lacZ mRNA had no effect. In 7 of 18 injected embryos, *fgf8* mRNA injection caused expanded *pax2.1* expression in the placodal region at the 12-somite stage. Fgf8 is thus sufficient to stimulate *pax2.1* expression ectopically. However, the ability to turn on *pax2.1* ectopically in response to Fgf8 misexpression is limited to the ectoderm adjacent to the posterior hindbrain rhombomeres (Figs. 6B,C). Likewise, Fgf8 beads implanted at shield stage ( $n = 3/14$  that ended up in the hindbrain/otic region) were able to induce expanded ear vesicles in wild-type embryos (Fig. 6E), that expressed *sprouty4*, a target gene for Fgf8 signalling, in its normal position at the anterior vesicle pole (Figs. 6F,G). We have however not observed additional ear vesicles in such embryos, suggesting that Fgf8 may act in conjunction with other signals.

### 2.8. *Fgf8* is required in the adjacent hindbrain for placode induction

While our mRNA injection and bead implantation experiments showed an expansion of otic territory in response to Fgf8, they did not allow us to address the mechanisms or the normal source of Fgf8 signaling. To test more directly whether Fgf8 emanating from r4 to 6 is responsible for placode induction, we transplanted wild-type cells into the hindbrain primordium of *ace*<sup>-</sup> mutants at pregastrula stages. The resulting chimaeras were stained for *pax2.1* as a placode marker, and with  $\beta$ gal-antibody to detect the location of the transplanted cells (Figs. 7A,B). *pax2.1* staining is also reduced at the MHB in the mutants (Reifers et al., 1998), allowing us to distinguish wild-type and *ace*<sup>-</sup>

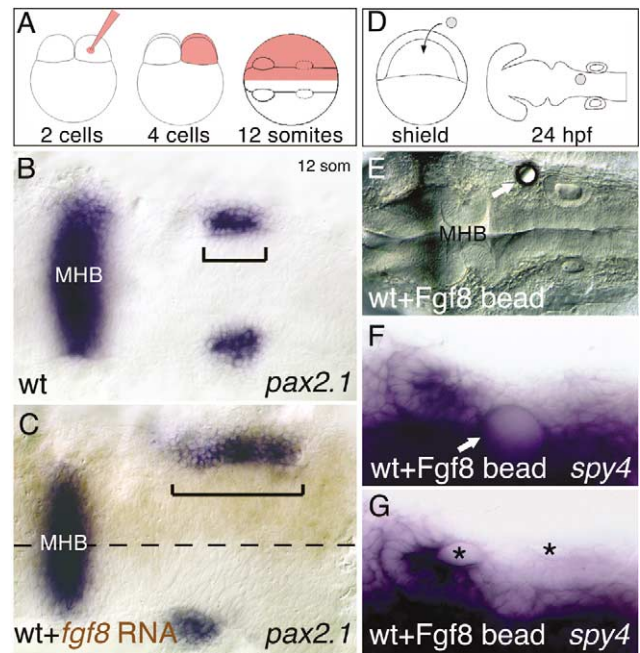
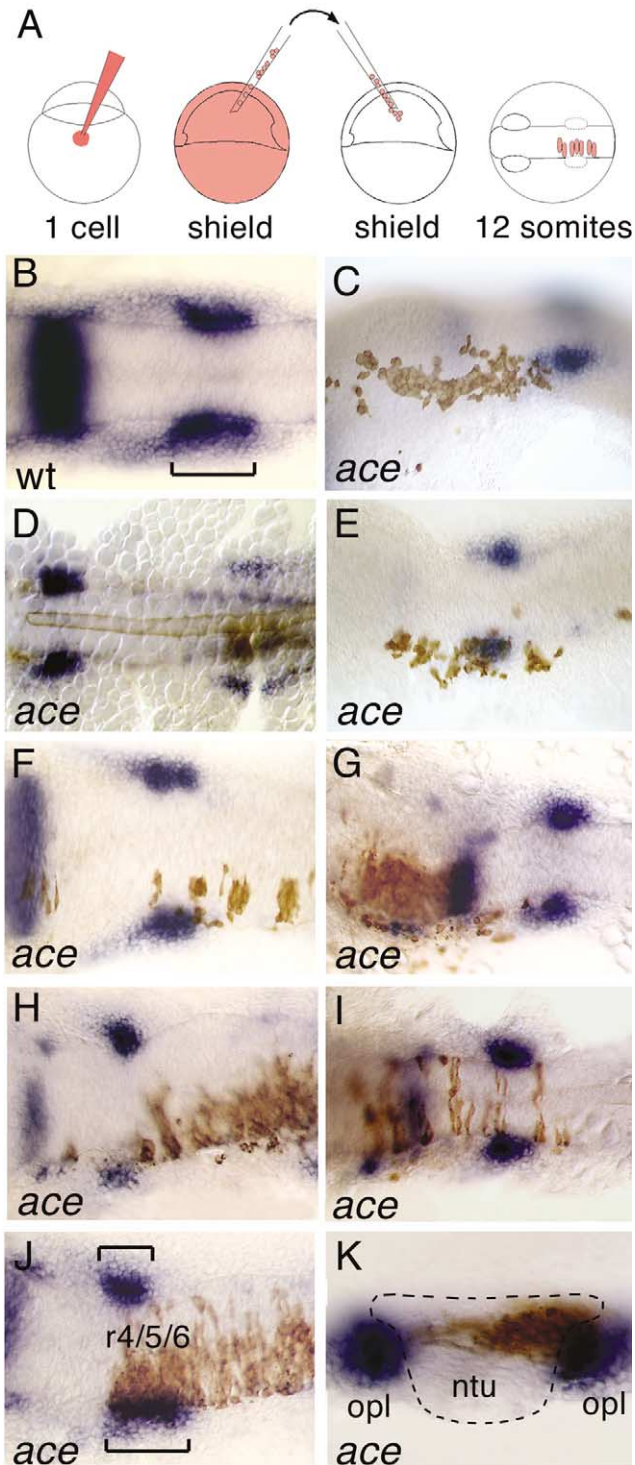


Fig. 6. Fgf8 misexpression expands *pax2.1* positive territory in competent cells next the hindbrain. (A) Co-injection of *fgf8* and lacZ mRNAs in wild type embryos at the 2-cell stage creates chimaeric embryos misexpressing *fgf8* on one side, which are then examined for *pax2.1* expression. (B, C) Expression of *pax2.1* (ISH) in the otic primordium (bracket) of a wild-type embryo and a unilaterally injected embryo; the injected cells are located in the right half of the embryo, as revealed by the antibody to  $\beta$ -gal (brown) at the 12-somite stage, dorsal views. Note the expansion of the *pax2.1* positive otic expression domain on the injected side in (C), indicated by a long bracket, compared to the uninjected side, or the wild-type embryo in (B). The midline is indicated by a dashed line. (D) A heparin bead covered with Fgf8 is implanted into the hindbrain primordium of wild type embryos at the shield stage, prior to placode formation. The effects are scored on otic vesicle formation, and on activation of the Fgf target gene *sprouty4*. (E) Live embryo at 30hpf that had received an Fgf8 bead; note the enlarged ear vesicle on the side of the bead (arrow). (F, G) *sprouty4* expression (ISH) at the anterior pole of an enlarged, partially split ear vesicle at the 20-somite stage. The split was observed in two cases out of three; the enlarged ear apparently split secondarily, probably due to the mechanical hindrance of the bead. Two focal planes of the same embryo showing the bead (F, arrow) and the two lumina of the partially split otic vesicle (G, \*). Dorsal views. MHB, midbrain-hindbrain-boundary.

chimaeric embryos. When wild type cells were located in the mesoderm, notochord, ectoderm or in the hindbrain anterior to or posterior to r4–6, no rescue was observed (Figs. 7C–I). A chimaera was scored as ‘rescued’ when the size of placodal *pax2.1* expression in *ace*<sup>-</sup> mutants was restored to wild-type size. Using this stringent criterion, rescue was observed in two chimaeras out of 31 with clones located in the hindbrain of *ace* mutants. In both cases, many (more than about 40) transplanted wild-type cells were located adjacent to the site of placode formation in hindbrain rhombomeres 4–6 (Fig. 7J). Two additional clones with few (<10) cells in r4–6 did not show visible rescue (Fig. 7I), nor did four clones with cells in the otic placode itself (Figs. 7E,F). In a cross-section of the hindbrain-clone in Fig. 7J we observed transplanted cells only in the hindbrain

neuroepithelium, but not in the underlying endo- or mesoderm, nor in the otic placode itself (Fig. 7K), although we are normally able to detect overlapping labeling in the placode, and observed a clear separation between the labeled neural tube cells and the placode prior to flattening of the embryo for the photograph in Fig. 7J. These results strongly suggest that Fgf8 emanating from r4 to 6 during early somitogenesis stages acts to induce otic placode development.



To address the importance of endomesoderm as a source for otic inducers further, we examined embryos lacking cephalic endomesoderm because they are defective in nodal signaling, due to lack of maternal and zygotic *one-eyed pinhead* product, a crucial cofactor in Nodal signaling (*mzoep* embryos; Gritsman et al., 1999; Schier and Shen, 2000). We find that in *mzoep* embryos otic vesicles do form and express *otx1* regionally, although they are typically of abnormal shape (Figs. 8A,B,M,N). The placode markers *pax8*, *pax2.1* and *dlx3* are activated in normal spatial relation to the forming rhombomeres stained with *krox20* (Figs. 8C–H); however, marker expression is seen at more medial levels from tailbud stages onwards. Because midline tissue is absent develops abnormally in these embryos, this may reflect a repressive influence of the midline on the medio-lateral extent of the otic primordium. In the early hindbrain primordium of *mzoep* embryos, *fgf8* and *fgf3* are initially activated properly, and *fgf3*, but not *fgf8* expression is maintained in rhombomere 4 (Figs. 8I–L). Consistent with the results of our transplantation experiments, these findings show that otic induction can proceed in the absence of developing endomesoderm.

### 2.9. Successive requirements for Fgf signaling

To confirm the importance of Fgf signaling in otic induction, and to resolve temporal aspects, we treated wild-type embryos for different periods with the pharmacological inhibitor SU5402, which is thought to block all Fgf receptor signal transduction (Mohammadi et al., 1997). The phenotype of living inhibitor-treated embryos closely resembles that of *ace*<sup>-</sup> mutants with respect to the developing inner ear, midbrain-hindbrain boundary and heart (Figs. 9A–C; Reifers et al., 2000a; Araki and Brand, 2001). We treated embryos for different periods of development and find that Fgf signaling is absolutely required for inner ear induction, and that there is a separate requirement during later differentiation. We used *sprouty4* to confirm that the inhibition was complete (Figs. 9D,E,L,M). Inhibition starting at 70% epiboly, the tailbud or the 2-somite stage, results in complete loss or strong reduction of the expression of *pax8*, *pax2.1* and *dlx3* (Figs. 9F–K; Table 1), resulting in

Fig. 7. Fgf8 is required in the adjacent hindbrain for placode induction. (A) Fluorescently labelled wild-type cells were transplanted into the primordia of different tissues of *ace*<sup>-</sup> embryos at shield stage, and the ability to rescue the normal extend of placode formation was assayed by ISH. (B–K) Expression of *pax2.1* (ISH) at the 12-somite stage. (B) wild-type embryo. (C–I) *ace*<sup>-</sup> chimeras carrying transplanted cells (brown) in the mesoderm. (C), in the mesoderm (C), in the notochord and the trunk (D), in the otic primordium itself (E, F), in the midbrain and the mesoderm (G) in the posterior hindbrain (H) and in the midbrain and the hindbrain (few cells) (I). (J) Rescue of the *pax2.1* expression in the otic primordium (bracket) in an *ace*<sup>-</sup> chimera carrying many transplanted cells (more than 40) in the hindbrain adjacent to the otic domain. (K) Transverse section at the level of the otic primordium in the chimera shown in (J). Dorsal views, except (C, K), lateral views. (r4) rhombomere 4, (opl) otic placode, (ntu) neural tube.

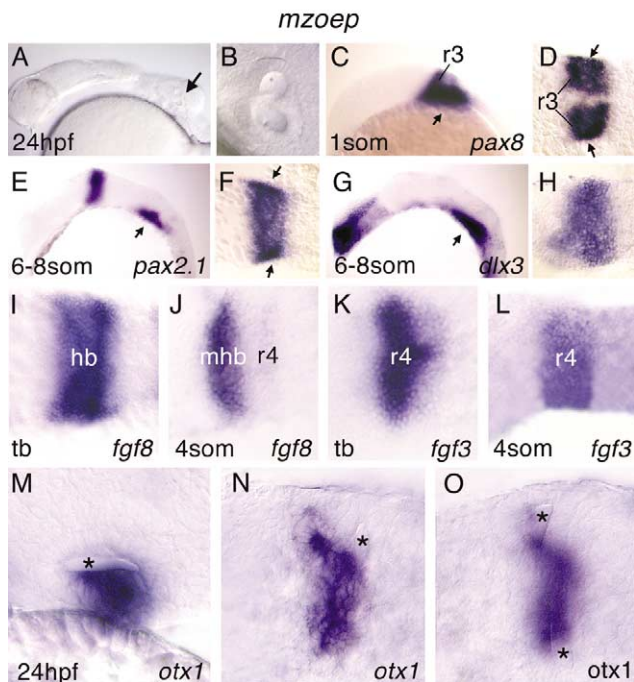


Fig. 8. Depletion of cephalic endomesoderm in *mzoep* embryos devoid of Nodal signaling still allows normal placode induction. (A, B) Live phenotype of *mzoep* embryos around 24 hpf, lateral views; otic vesicles form in spite of the distorted anatomy of these embryos. (B) Closer view of a partially split vesicle shown in (A). (C–H) Early expression of *pax8*, *pax2.1* and *dlx3* in the otic primordium (arrow) of *mzoep* embryos (stages and markers as indicated). (D, F, H) Dorsal views of the lateral views shown in (C, E, G), respectively. (I–L) Expression of *fgf8* (I, J) and *fgf3* (K, L) in the hindbrain of *mzoep* embryos at the tail bud-stage and the 4-somite stage, as indicated. Dorsal views. (M–O) *Otx1* expression in the otic vesicle of *mzoep* embryos at 24 h. (M) Lateral view. (N, O) Dorsal views of the same embryo shown in (M), taken at two different focal planes. Notice that *otx1* expression stretches across the midline, showing one large otic vesicle stretching across the midline, or several interconnected smaller vesicles, that form in *mzoep* embryos. (\*) lumen of the otic vesicle. (r3), (r4) and (r5) rhombomeres 3, 4 and 5, respectively, (mhb) midbrain-hindbrain-boundary, (hb) hindbrain.

very tiny or no ears after 24 h (Figs. 9B,C). *pax8* and *pax2.1* staining is absent in Fgf-inhibited embryos, and *dlx3* is not upregulated in the otic region. Treatment for different times between the tailbud- and 18-somite stage reveals that Fgf signaling is not only required for induction, but also required to maintain expression of *pax8*, *pax2.1* and *dlx3* in the otic placode (Table 1). In contrast, inhibition after the 18-somite stage up to 24 h has no effect on *pax2.1* and *dlx3* (Figs. 9N–Q); *pax8* is downregulated in the otic vesicle after the 10 somite-stage. Thus, between the 1 and 18 somite-stage Fgf signaling is critically required for induction and maintenance of otic placode markers.

To test whether Fgf signaling acts again during the vesicle stage, as the *fgf8* expression pattern and the phenotype of *ace*<sup>-</sup> mutants suggested, we inhibited wild-type embryos during otic vesicle development, after the 18-somite stage. *sprouty4*, *pax5*, *otx1*, *gsc*, *msxC* and *mshD* expression is specifically lost from the otic vesicle, with no apparent

reduction of vesicle size (Figs. 4D,H,L,P,T, 5D and 9L,M; Table 1), whereas expression of *neurogenin1* and *snail2* is not affected (Fig. 4T, and not shown). These observations, together with the analysis of the expression pattern and the *ace*<sup>-</sup> phenotype, show that Fgfs in general, and Fgf8 in particular, function during otic induction and again independently during vesicle stages.

#### 2.10. *Fgf3* acts together with *Fgf8* in ear induction

Fgf inhibition also results in phenotypes that are often stronger and less variable than the *ace*<sup>-</sup> phenotype, suggesting that other Fgfs are involved in inner ear development in addition to Fgf8. Consistent with this possibility we find that *fgf3* (Kiefer et al., 1996) is co-expressed with *fgf8* from 85 to 90% epiboly onwards in the hindbrain primordium. Expression is seen initially in a single broad domain in the posterior hindbrain primordium, that at the 2-somite stage becomes confined to r4 where it remains expressed until the 18-somite stage; expression is downregulated by 21 h (Figs. 10A–D; Phillips et al., 2001; Maroon et al., 2002). Moreover, *fgf3*, *fgf8* and *fgf17* (Reifers et al., 2000b) are co-expressed in the anterior macula at vesicle stages (Figs. 10E–H). Consistent with the notion of redundancy, *fgf3* is expressed independently of *acelfgf8* during gastrulation and somitogenesis stages (Fig. 10D), and *fgf3* and *fgf17* expres-

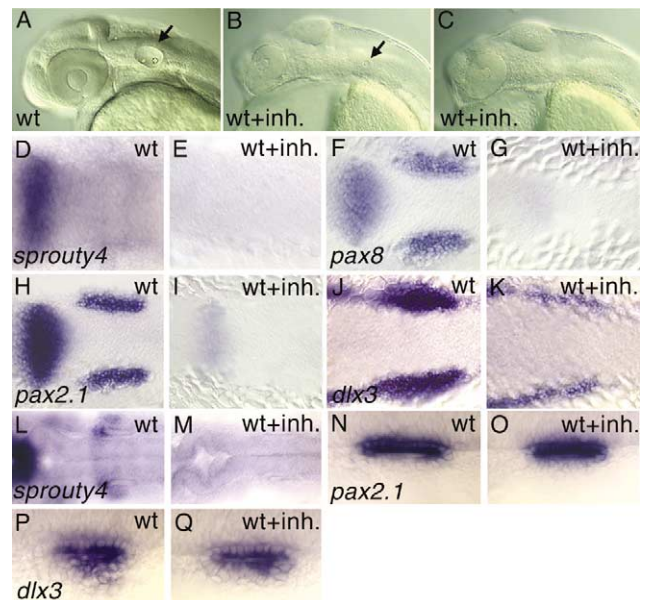


Fig. 9. Pharmacological inhibition of Fgf signaling with the SU5402 inhibitor during otic induction and otic vesicle patterning. See also Table 1. (A, K) Inhibition during placodal induction. (A, C). Live phenotype at 30 hpf of a wild-type embryo (A) and wild-type embryos inhibited from the tail bud stage onwards (B, C). Lateral views. (D–K) ISH, expression at the 6-somite stage of *sprouty4* (D, E) and early otic markers (F–K, as indicated) in wild-type embryos and wild-type embryos inhibited from the tail bud-stage to the 6-somite stage, as indicated. Dorsal views. (L–Q) Inhibition at the vesicle stage. Expression at 24 hpf of *sprouty4* (L, M) and early otic markers (N–Q, as indicated) in wild-type embryos and wild-type embryos inhibited from the 18-somite stage to 24 hpf, as indicated. Dorsal views.

Table 1  
Temporal requirement of Fgf signaling

	Inhibition at placodal stages						Inhibition at vesicle stages	
	70–95%	tb–4 s	4–6 s	6–9 s	10–15 s	14–18 s	18 s–24 h	24–48 h
Otic marker expression								
<i>pax8</i>	Absent	Absent	Absent	Absent				
<i>pax2.1</i>		Absent	Absent	Reduced	Reduced	Weakly reduced	Wild type	
<i>dlx3</i>		Absent	Absent	Absent	Reduced	Weakly reduced	Wild type	
<i>pax5; mshD otx1; goosecoid</i>							Absent	
<i>neurogenin1; snail2; six4.1</i>							Wild type	
<i>mshC</i>								Absent

sion is reduced, but present in *ace*<sup>-</sup> ears at later stages (Figs. 10F,H).

To test the notion of redundant Fgf functions further, we determined the function of *fgf3* in ear development, by injecting morpholino antisense oligonucleotides (Nasevicius and Ekker, 2000; Mo-*fgf3* and Mo-*fgf8*) into wild-type and into *ace* mutant embryos. We find evidence that *fgf3* and *fgf8* are both required for placode induction (Figs. 10I–Z, Table 2). Injection of 10 or 15 ng of Mo-*fgf3* into wild-type embryos causes a reduction of both ear size and gene expression of the otic markers *pax8*, *pax2.1*, *dlx3*, *pax5*, *mshD*, *msxC*, *otx1*, *goosecoid* and *neurogenin1*, similar to, and at later stages stronger than that observed for *ace* mutants (Figs. 4C,G,K,O,S, 5C,D and 10M–P, and not shown). At late gastrula stages and 24 h, *fgf8* expression is unaffected in these embryos (Figs. 10Y,Z). In addition, Mo-*fgf3* injection causes absence of all epithelial protrusions of the semicircular canals (not shown); further defects are seen in early forebrain development (Raible and Brand, 2001). Control injections with 15 ng of a four-basepair-mismatched morpholino, or a random sequence morpholino, or of morpholinos directed against a number of unrelated genes, have no such effects (Table 2 and not shown). To test the idea of a possible redundancy between Fgf8 and Fgf3, we co-injected embryos with Mo-*fgf3* and Mo-*fgf8*, which causes either very strong reduction or complete absence of the ear vesicle ( $n = 73$  absent of 96 injected; of the remaining 23 ears, 21 were reduced to about half the size, and two were wild type; Table 2, Figs. 10Q,R). The same phenotype is observed for *ace* mutants injected with Mo-*fgf3* ( $n = 20$  of 20; Table 1; Figs. 9U,V). Expression of *pax8* and *pax2.1* during placode induction stages is absent or very strongly reduced under those conditions ( $n = 33$  of 38; Figs. 9S,T,W,X). As expected, and as we observed in inhibitor treated embryos, the expression of *dlx3* and *eyal* is not affected initially, but fails to be maintained after the placode induction stage in these embryos (not shown). Thus, Fgf3 and Fgf8 redundantly specify placode induction.

### 3. Discussion

Classical transplantation studies have provided evidence for the existence for a hindbrain-derived signal involved in

induction of the ear placode, but the nature of the signal itself, its time of action, whether it serves an inductive or permissive role, and through which downstream target genes it acts have been enigmatic. Our results partly confirm and extend, but also differ in some aspects (see below) from those of two independent reports by Phillips et al. (2001) and Maroon et al. (2002), describing redundant functions of

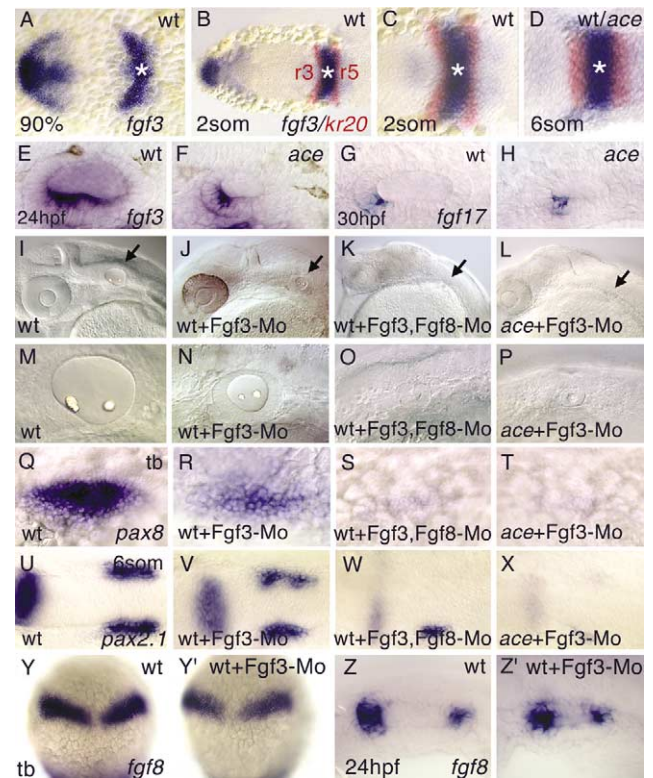


Fig. 10. Fgf3 acts together with Fgf8 in otic induction and differentiation. (A–D) Expression of *fgf3* in the hindbrain (\*) during placode induction (stages as indicated) in wild-type (A–D) and *ace* (D) embryos. (B–D) Double ISH with *krox20* (red). (r3) and (r5) rhombomeres 3 and 5 respectively. (E–H) Expression of *fgf3* (E, F) and *fgf17* (G, H) in the otic vesicle at 24 hpf in wild-type and *ace* embryos, as indicated. (I–Z) Morpholinos injection. Live phenotype at 30 hpf (I–P) and early otic marker expression (Q–X, stages and markers as indicated) in wild-type and *ace* embryos, wild-type embryos injected with Mo-*fgf8* and Mo-*fgf3* and *ace* embryos injected with Mo-*fgf3*, as indicated. (Y–Z') *fgf8* expression in the hindbrain (Y, Y') and in the otic vesicle (Z, Z') is normal in wild type embryos injected with Mo-*fgf3*.

Table 2  
Fgf3 and Fgf8 are required for otic induction

		No ear	Tiny ears	Reduced ear size <sup>a</sup>	Wild-type ears	Total number
Mo- <i>fgf3</i>	15 ng Mo- <i>fgf3</i>	0	0	92 <sup>b</sup>	0	92
Mo- <i>fgf3</i> -MM	15 ng	0	0	0	92	92
Mo- <i>fgf3</i> + Mo- <i>fgf8</i>	10 ng Mo- <i>fgf3</i> + 4 ng Mo- <i>fgf8</i>	0	41	21	2	64
	15 ng Mo- <i>fgf3</i> + 8 ng Mo- <i>fgf8</i>	n.a. <sup>c</sup>	32	0	0	32
<i>ace</i> <sup>-</sup> + Mo- <i>fgf3</i>	10 ng Mo- <i>fgf3</i>	10	10	0	0	20

<sup>a</sup> Size as seen in *ace* mutants.

<sup>b</sup> All ears had two otoliths.

<sup>c</sup> In these injections more than 50% of the embryos do not develop to the ear vesicle stage. When assayed for *pax2.1* expression at eight somites, 18 of 21 embryos had no *pax2.1* expression in the ear placode. Control injections with a four pair-base mismatch morpholino against *fgf3* or *fgf8* (Araki and Brand, 2001), and a random sequence morpholino have no effect on ear development.

Fgf8 and Fgf3 in otic induction. Our work provides consistent evidence from expression studies, cell transplantations, gain-of-function experiments, loss-of-function analysis of *acerebellar/fgf8* mutants, pharmacological inhibition of Fgf-signaling and morpholino-inactivation of *fgf3* and *fgf8*. This evidence suggests that Fgf8 and Fgf3 are the molecules mediating activity of the endogenous hindbrain-derived ear inducer, acting in a redundant fashion during the earliest stages of placode induction. Furthermore, we find that Fgf8 and Fgf3 serve additional function(s) in patterning and differentiation of the otic vesicle at later stages. Whereas our results strongly argue that Fgf3 and Fgf8 act as hindbrain-derived signals, our analysis of *mzoep* embryos lacking cephalic endomesoderm does not support a major role of this tissue in otic induction.

### 3.1. The initial stage of otic induction requires Fgf8 and Fgf3 signaling from the hindbrain primordium

Transfilter experiments have suggested that the induction of the inner ear by the neural tube is due to a diffusible molecule from the neural tube, rather than direct cell-cell contact (Van de Water and Conley, 1982). Fgf3 and Fgf8 are thought to encode secreted factors, which fits with their proposed role to mediate the hindbrain action on inner ear development. Our analysis of *acerebellar/fgf8* and *fgf3* function provides clear evidence for an Fgf requirement as a signal acting from the hindbrain: (i) during placodal induction, *fgf8* and *fgf3* are not expressed in the placode itself, but the expression in the hindbrain during late gastrulation/early somitogenesis-stages fits the expected timing and tissue distribution of the signal. (ii) The expression of placode marker gene expression is reduced to about half the size when *fgf3* or *fgf8* are singly inactivated, and completely lost when both are inactivated. At otic vesicle stages this results in smaller otic vesicles of the *ace* mutants or *fgf3*-morphants. This clearly demonstrates the requirement for Fgf3 and Fgf8 at the appropriate stage for induction. (iii) More generally, our SU5402 inhibition experiments are

consistent with an involvement of Fgfs as signals specifically during late-gastrulation to early-somitogenesis stages, the time of initial otic induction. Importantly, inhibition during this period leads, in our hands, to complete loss of otic induction as observed by *pax2.1*, *dlx3* and *pax8* expression, whereas Maroon et al. (2002) report that expression of *pax8* is not affected until the 2–3 somite stage. The reasons for this different finding is not clear, but we tentatively suggest a lower effective concentration of SU5402 may have been employed by these authors. Alternatively, it may matter whether Fgf signaling is blocked starting at 30% epiboly, as reported by Maroon et al., or from 70% of epiboly (our work), shortly before onset of the endogenous *pax8* expression. We were not able to obtain reliable development of embryos when FGF inhibition was started at 30%, due to an independent requirement for Fgf signaling in maintaining early mesoderm development. Phillips et al. (2001) did not study the effects of SU5402 inhibition. We also observe complete loss of *pax8* expression when *fgf3* and *fgf8* are knocked-down via morpholino-injection, as is also reported by Phillips et al. (2001), and, for one embryo, also by Maroon et al. (2002). Together, these results argue that already the first stage of placode induction requires Fgf3 + Fgf8 signaling. Examination of another target gene for Fgf8-signaling during gastrulation, *gbx2*, after SU5402 inhibition further supports this notion: *gbx2* is expressed from tailbud-stage onwards in the otic primordium, only slightly later than *pax8*, and is completely dependent on Fgf signaling (Reim and Brand, 2002; M. Rhinn, K. Lun and M.B., unpublished). (iv) Our transplantation chimaeras show that the hindbrain primordium, and in particular r4–6, is the site where wild-type activity of Fgf8 is needed for normal otic induction to occur. Fgf8 is also expressed in the mesendodermal primordium during gastrulation, called the germring, and during early somitogenesis in the lateral plate mesoderm and in the heart field, i.e. close to the forming otic placode (Reifers et al., 1998, 2000a). In accordance with our findings, grafts of rhombomere 4 indicate that this rhombomere carries the capacity of the hindbrain to induce the inner

ear (Sechrist et al., 1994). Transplantation experiments in chick and amphibians suggested that endomesoderm also has otic inducing capacity in the absence of hindbrain tissue (reviewed in Baker and Bronner-Fraser, 2001). For instance, in amphibian embryos cardiac mesoderm can act as a source for otic placode specifying signals (Harrison, 1935). However, in our transplantation chimaeras, wild type cells located in the mesoderm did not rescue the otic induction defect in *ace* mutants, although it remains formally possible that a larger number of wild-type cells would be needed in the mesoderm to achieve rescue. However, although *fgf8* is expressed in the heart field, we do not detect expression there before the 3-somite stage (Reifers et al., 2000a), i.e. after the onset of ear placode induction. The Fgf8 signal responsible for otic specification around the tail bud stage is therefore unlikely to come from the lateral plate mesoderm. Harrison's observation could however be explained by assuming that heart tissue, due to its Fgf8 expression, can under certain conditions mimic the activity of the endogenous hindbrain-derived Fgf8, in analogy to what was suggested to explain the ability of olfactory placode tissue (an unlikely endogenous inducing tissue) to induce limb formation (Slack, 1995).

### 3.2. Otic induction and *fgf3* and *fgf8* expression occur normally in embryos depleted of endomesoderm

In zebrafish, several mutants affecting early mesoderm development, including mutants lacking chordamesoderm, develop normal otic vesicles, whereas a slight temporal delay can be observed for others (Mendonsa and Riley, 1999). Specifically, morpholino-inactivation of the Nodal-cofactor *Oep* was reported to strongly delay *pax8* expression in the otic primordium in a portion of the embryos to the six-somite stage (Phillips et al., 2001). Because morpholinos can cause unspecific side effects, we used in our experiments *mzoep* embryos to inactivate both the maternal and the zygotic function of *oep* genetically by homozygosity for an *oep* null allele (Gritsman et al., 1999), which should formally give the same result as the morpholino injections. However, in *mzoep* embryos, which lack cephalic endomesoderm, we did not observe the strong delay of *pax8* expression reported by Phillips et al. (2001), nor of the other early placodal markers *pax2.1* and *dlx3*. Instead, we observe a normal temporal and spatial correlation of their expression sites, and hence the site of placode formation, in relation to the hindbrain. Therefore, genetic depletion of cephalic endomesoderm in *mzoep* embryos does not suppress otic induction. In addition, we observe normal expression of *fgf8* and *fgf3* in the early hindbrain of *mzoep* embryos, which we suggest to be the explanation for normal otic induction in these embryos. We do however observe a medial expansion of otic marker expression, suggestive of a lack of inhibitory signals from the midline, and it will be interesting to determine if this a direct or an indirect effect of Nodal signaling. Overall, our analysis of *mzoep* embryos

supports the notion derived from our transplantation analysis, that mesendoderm is unlikely to be a major source for the otic inducing signal missing in *acerebellar* mutants or *fgf3* + *fgf8* singly- or doubly-inhibited embryos. The endomesodermal primordium may however indirectly influence the formation of the otic primordium, e.g. by controlling patterning of the gastrula neuroectoderm.

### 3.3. *Fgf3* as a redundant signal with *Fgf8*

In spite of the important and early function of Fgf8 in ear induction, *acerebellar* mutants do have an, albeit smaller, ear, and placodal marker gene expression is reduced to about 50% of the size of the wild type placode. Why? Importantly, blockade of all Fgf signaling by SU5402 inhibition results in the formation of tiny ears, but more typically of no ear at all, suggesting that additional Fgfs are important for otic induction. As reported by Phillips et al. (2001) and Maroon et al. (2002), we find that Fgf3 acts redundantly with Fgf8. *fgf3* is also expressed in hindbrain rhombomere 4 from 85 to 90% of epiboly onwards, and its expression is normal in *ace* mutants. Fgf3 is therefore available to partially compensate the lack of Fgf8 in *ace* mutants, and the results of the joint depletion of Fgf8 and Fgf3 suggests this is indeed the case.

In other species Fgf3 (int-2) is involved in inner ear development, but its precise role is unclear. Expression studies in mouse, chicken and *Xenopus* demonstrate the presence of *fgf3* in the hindbrain, close to the otic domain at early somite stages (Wilkinson et al., 1988; Tannahill et al., 1992; Mahmood et al., 1995); our studies on *fgf3* expression confirm this notion for the zebrafish gene. Functional studies for *fgf3* have however given conflicting results. Consistent with a requirement for Fgf3, *Hoxa-1* (*Hox1.6*) mutant mice show a delayed formation and gross morphological alteration of the otic vesicle (Chisaka et al., 1992; Dolle et al., 1993; Lufkin et al., 1991), and also have reduced Fgf3 expression (Mark et al., 1993; McKay et al., 1994). Moreover, Fgf3 antisense oligonucleotides and anti-Fgf3 antibody inhibit the formation of chick otic vesicles (Represa et al., 1991). More recently, overexpression in chick showed that *fgf3* is capable of mimicking the activity mediating early induction (Vendrell et al., 2000). Conceivably, however, the antibody used in this study might also inhibit other members of the Fgf family. Furthermore, targeted disruption of *fgf3* in mice does not lead to absence or reduction of the otocyst, but rather affects the differentiation of the otocyst with incomplete penetrance (Mansour et al., 1993). One possibility is that in gain-of-function situations, Fgf3 mimics all or part of the activity of another Fgf. Our studies on Fgf3 function are consistent with a requirement for Fgf3 in otic induction, but with an important difference. As previously suggested (Kinoshita et al., 1995; Mansour et al., 1993) also for other tissues (Fürthauer et al., 2001; Raible and Brand, 2001; Reifers et al., 2000b), functional redundancy between different Fgf's is a likely

explanation: our results show that the full phenotypic requirement, visible as absence of otic vesicle formation and lack of early placodal marker expression, only becomes apparent when Fgf8 and Fgf3 are both inactivated, either through mutation, or by co-injection of morpholinos. Given that the double-inactivated embryos show the same phenotype as the SU5402 inhibited embryos, Fgf3 and Fgf8 together probably account for a large portion or all of the hindbrain-derived placode inducing activity. Interestingly, expression of Fgf8 in the early hindbrain primordium has not been reported in mice and chick, raising the possibility that in these animals another Fgf cooperates with Fgf3 in ear induction, such as Fgf4, which is expressed in the early neuroectoderm in chick (Shamim and Mason, 1999). Additional Fgfs or other signaling molecules may serve additional functions, for instance Fgf19 might act as a paraxial mesoderm-derived signal in chick otic placode induction; the timing of expression from the 6-somite stage onwards suggests this may be a function following the initial induction (Ladher et al., 2000). The different phenotypes we observe following *fgf8* inactivation and *fgf3* inactivation in zebrafish suggests that the two components of the inducing signal are not identical; we have not addressed whether the difference is merely quantitative or also qualitative in nature. Interestingly, Fgf8 bead implantations in chick indicate that not all otic placode markers can be equally activated ectopically in response to Fgf8 alone (Adamska et al., 2001). Our results suggest that simultaneous expression of Fgf8 and Fgf3, and possibly other factors, is necessary for ectopic activation of the full ear program.

The spatial limitation of the site of placode formation may largely be due to the hindbrain derived Fgf signal, including Fgf8 and Fgf3. A key question is whether Fgf3 and Fgf8 act directly, or via a relay mechanism on preplacodal ectoderm. Several studies demonstrate that Fgf8 is also needed for normal patterning events in the hindbrain around the time of placode induction (Fürthauer et al., 2001; Raible and Brand, 2001; Maves et al., 2002; Reim and Brand, 2002). Our finding that two ETS-type transcription factors acting downstream of Fgf signaling require Fgf8 for their expression in the ear placode (Raible and Brand, 2001) favours in addition the possibility of a direct action. Furthermore, FgfR1, as the likely receptor for Fgf8 (Fürthauer et al., 2001) is expressed in the ear (unpublished observations), as are FgfR2 and FgfR4 (C. Thisse and B. Thisse, personal communication). Although we did not assay for Fgf3 and Fgf8 protein directly, these proteins are presumably present in limiting quantities during ear induction, since our gain of function experiments either with RNA injection, or with bead implantation, could clearly expand the size of the area where otic placode is formed. The area responding to Fgf exposure in our experiments is however limited, defining a zone of competence, which appears to be restricted to a stripe of cells adjacent to the hindbrain. A similar restricted competence was observed for the response to Fgf3 bead implantation in

chick (Vendrell et al., 2000), suggesting that the ability to generate an otic placode in response to Fgf signals is generally limited; see also Baker and Bronner-Fraser (2001), for further discussion on competence.

### 3.4. A model for Fgf function during early zebrafish ear development

We propose the following sequence of events for Fgf-dependent induction and patterning of the zebrafish inner ear (Fig. 11).

#### 3.4.1. Induction phase

Initially, the entire ventral cephalic ectoderm is competent to respond to placode inducing signals, but competence becomes increasingly restricted (Gallagher et al., 1996; Groves and Bronner-Fraser, 2000; Yntema, 1950). Our analysis similarly suggest that the cells responding to Fgf signals are to some extent pre-specified. *dlx3*, *eya1* and *six4.1* are initially expressed in a stripe of cells at the neural-non-neural ectoderm border that gives rise to several placodes (Akimenko et al., 1994; Kobayashi, 2000; Sahly et al., 1999), and this expression is not affected by absence of Fgf8 and Fgf3. During otic induction, the placode appears to form from within this stripe (Fig. 11), concomitant with upregulation of the above genes, and the placode-specific expression of markers like *pax8* and *pax2.1*. At more anterior levels, the olfactory placode is thought to arise from the same stripe (Whitlock and Westerfield, 2000). These genes are therefore good candidates to define a state of multiplacodal competence (Jacobson, 1963a, and discussion in Baker and Bronner-Fraser, 2001). Importantly, upregulation of *dlx3* and *eya1* in the otic region fails to occur in the absence of Fgf8 and Fgf3 signaling, suggesting that the transition from a competent to an induced state is deficient in the absence of Fgf8 and Fgf3. This transition does not require the presence of cephalic endomesoderm and its derivatives. We therefore suggest that ear placode is specified after definition of the multiplacodal ground state, with Fgf3 and Fgf8 together defining the signal allowing transition to an otic placode. In agreement with this model, the acquisition of placodal competence is thought to start in the early gastrula or in the midgastrula stage (Gallagher et al., 1996; Jacobson, 1963a; Servetnick and Grainger, 1991). Then, as otic field specification occurs, the placodal competence becomes restricted to the prospective ear region (Gallagher et al., 1996; Zwilling, 1941).

#### 3.4.2. Maintenance phase: Fgf's in patterning and differentiation of the otic vesicle

At induction, placode markers like *pax2.1*, *pax8*, *eya1*, *dlx3* and *six4.1* show relatively uniform expression throughout the placode primordium, arguing that initially there is no distinction between subregions of the placode. After going through this uniform otic ground state, the otic placode becomes polarized, visible for instance by the polar expres-

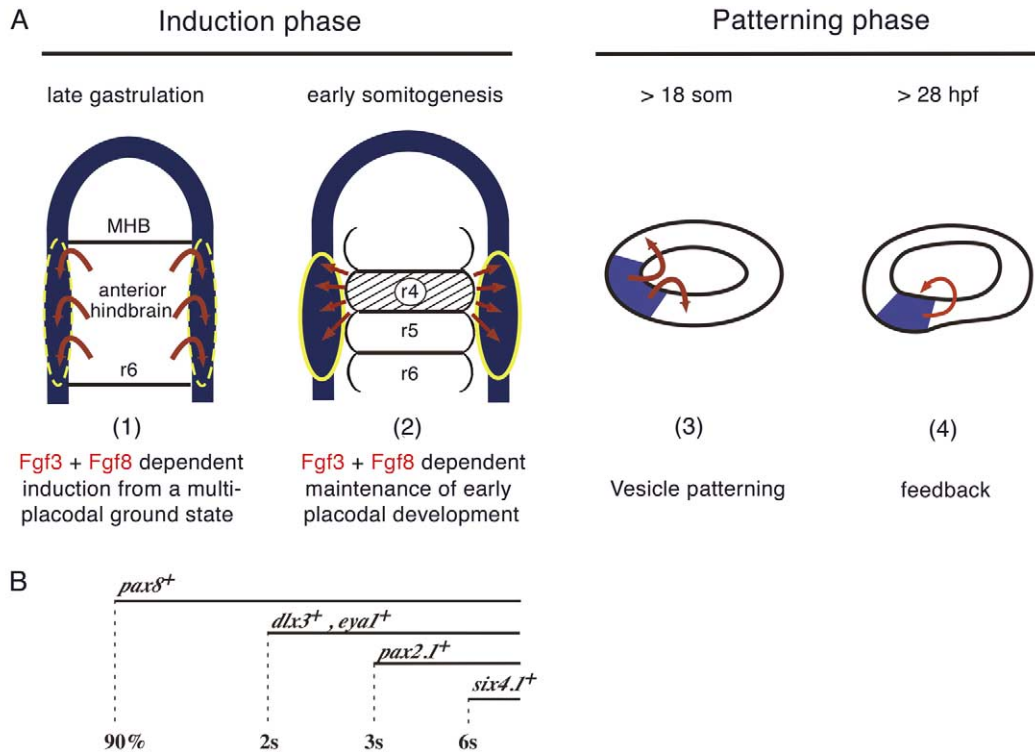


Fig. 11. Fgf function and inductive events during successive steps of zebrafish inner ear induction and patterning. (A) During the induction phase (1), the otic placode is induced within the domain of multiplacodal competence by Fgf8 and Fgf3 acting from the hindbrain primordium, resulting in expression of otic placode markers in a specific temporal order (given in B). The domain of multiplacodal competence (expressing *dlx3*, *eya1* and *six4.1*) is indicated in blue. (2) Fgf3 and Fgf8 become successively restricted to rhombomere 4, and are required to maintain placodal development in its vicinity. (3) The otic vesicle is subdivided from an initially symmetric state during the patterning phase. Fgfs signal a second time from the anterior vesicle pole (dark blue, arrow) during the patterning phase of the otic vesicle, and (4) during feedback regulation in the anterior sensory macula. For further discussion see text.

sion of markers like *pax5*, *pax2.1*, *gsc*, *fgf8* and others at the vesicle stage. From comparison of gene expression domains at this stage, it has been suggested that these domains might provide the information needed to confer positional information and a cell-type specification code for sense organs in the otic vesicle (Fekete, 1996), but it is unclear how the domains are initially set up and how they are further elaborated. Our results suggest that Fgf's in general, and Fgf8 and Fgf3 in particular, act a second time in setting up this pattern at the otic vesicle stage. Fgf8 and Fgf3 expression is now detected for the first time in the otic vesicle, at the anterior pole and, for Fgf8 very weakly and transiently, at the posterior pole. This symmetric *fgf8* expression is more pronounced in *ace* mutant vesicles, and *ace* mutants sometimes even show a fusion of the maculae (macula communis). We cannot rule out that this is simply the consequence of the reduced vesicle size. However, symmetrical arrangements with only two semicircular canal protrusions and with a macula communis is typical for the inner ears of the more primitive myxinooids, whereas the typical split maculae of higher vertebrates are first observed in *Petromyzontes* (Gegenbaur, 1898; Fritsch et al., 1998). The more symmetrical *ace* mutant phenotype might therefore reflect an atavistic condition of an otic vesicle with symmetric morphological traits. In teleosts a bipartite macula is

observed only rarely (e.g. in *Chimaera monstrosa*), three maculae being the more typical condition (Gegenbaur, 1898). The basis for this difference in ear organization is not known, but we tentatively suggest, in analogy to the MHB organizer (Sharman and Brand, 1998), that this involves the development of an ear organizer at the anterior pole of the ear vesicle that utilizes Fgf8, probably in conjunction with other Fgf's, as the signaling molecule. It is interesting to note that in both the MHB and ear vesicle, this also involves *otx1* gene function (Morsli et al., 1999), suggesting that part of the patterning machinery operating in development of the MHB organizer may also act during ear patterning. Ear specific inactivation of *fgf8* and *otx1* at this stage can be used to address their detailed functions in otic vesicle patterning and differentiation.

Expression of *fgf8*, *spry4*, as well as *erm* and *pea3* (Raible and Brand, 2001) correlates at the vesicle stage with defects in otic vesicle patterning, neurogenesis, and abnormal semicircular canal protrusions that we observed in the mutants. Due to the smaller size of the *ace* vesicle, aspects of these phenotypic traits are likely to be a secondary consequence of the size reduction. The selective inhibition with SU5402 at this stage (from 18 somite-stage onwards) has provided evidence both for such indirect effects, and for likely direct effects of Fgf signalling. Expression of *spry4*, *pax5*, *gsc*,

*mshD* and *otx1* is absent after inhibitor treatment, showing that Fgf signaling specifically acts at the vesicle stage in regional subdivision of the vesicle. Similarly, *msxC* expression in the crista epithelium is affected both in *ace* mutants and after inhibition. In contrast, *neurogenin1* and *snail2* (and *nkx5.1*; Adamska et al., 2000) expression is only affected in *ace* mutant vesicles, but not after late SU5402 inhibition, showing that the effect on reduction of the VIIIth ganglion is probably a secondary consequence of the reduced ear vesicle size in *ace* mutants. We therefore suggest that Fgf-dependent patterning of the otic vesicle starts during late somitogenesis/early pharyngula stages (Fig. 11), and requires Fgf8, probably in conjunction with other Fgf's, to achieve proper patterning of the otic vesicle. At otic vesicle stages additional Fgfs like Fgf17 and Fgf3 are expressed in the same ventro-anterior domain as Fgf8 (Reifers et al., 2000b; this paper). These *fgfs* are also not expressed in the ear before the vesicle stage, but may, as we have shown here during placode induction, cooperate with Fgf8 during otic vesicle differentiation. For instance, expression of Fgf8 is upregulated in *ace* mutant vesicles, probably reflecting the lack of feedback regulation in the mutants (Fürthauer et al., 2001; Reifers et al., 2000b), whereas *spry4* and *fgf3* are downregulated, and *fgf17* is unaffected (this paper). These data also provide further evidence that Fgf8 is still signaling at the vesicle stage, also in the developing macula, where its function remains to be determined.

#### 4. Experimental procedures

Zebrafish were raised and kept under standard laboratory conditions at about 27°C (Brand et al., 2002; Westerfield, 1994). To obtain *ace* mutant embryos, two heterozygous *ace<sup>iz282</sup>/+* carriers were crossed to one another. Typically, the eggs were spawned synchronously at dawn of the next morning, and embryos were collected, sorted, observed and fixed at different times of development at 28.5°C. In addition, morphological features were used to determine the stage of the embryos, as described by (Kimmel et al., 1995). In some cases, 0.2 mM phenylthiourea was added to prevent melanization. Isolation and characterization of *acerebellar* is described in Brand et al. (1996), Reifers et al. (1998) and Picker et al. (1999). A fraction of *ace<sup>-</sup>* larvae die due to abnormal heart development (Reifers et al., 2000a). For the behavioral studies, we therefore concentrated on larvae with relatively normal morphology and circulation. *Mzoep* embryos were obtained as described previously (Gritsman et al., 1999).

##### 4.1. *In situ* hybridization and histology

ISH were done as described in Reifers et al. (1998). Digoxigenin (DIG) labelled probes were prepared according to manufacturers instructions (Roche). Semithin sections

were cut at 1 µm and stained with toluidinblue/methylene-blue as described in Kuwada et al. (1990).

##### 4.2. Fluorescein-phalloidin staining of actin rich stereocilia

The following treatments were done at 4°C: 5 day old larvae were fixed in 4% paraformaldehyde (PFA) in phosphate buffered saline (PBS) for 2 days. They were then rinsed and permeabilized for 4 × 30 min in 2% Triton X-100 (Sigma) in PBS. Embryos were stained with 2.5 µg/ml fluorescein isothiocyanate (FITC)-labelled phalloidin (Sigma) in PBS for 2 h in the dark. The embryos were rinsed several times in PBS over 2 h and fixed in 4% PFA for half an hour and then rinsed in PBS. The ears were dissected out, mounted in PBS and viewed on a scanning confocal microscope.

##### 4.3. *Daspei* live staining of the lateral line hair cells

Five day old embryos were immersed in 1 mM DASPEI (2-(4-dimethyl-aminostyryl)-N-ethyl pyridinium iodide, Molecular Probes) in E2 for 1 h. They were then rinsed several times in E2, anaesthetized with tricaine (0.5 mM 3-aminobenzoic acid ethyl ester, 2 mM Na<sub>2</sub>HPO<sub>4</sub>), and mounted in methylcellulose for observation.

##### 4.4. RNA injections

*fgf8*, subcloned into pCS2+ (Rupp et al., 1994) was linearized and transcribed using the SP6 message machine kit (Ambion). The amount of RNA injected was estimated from the concentration and volume of a sphere of RNA injected into oil at the same pressure settings. Typically, about 25 µg of *fgf8* RNA were injected; RNA was dissolved in 0.25 M KCl with 0.2% of phenol red and backloaded into borosilicate capillaries prepared on a Sutter puller. During injection, RNA was deposited into the cytoplasm of two cells stage embryos; in embryos after the first cleavage, the RNA usually stays in the progeny of the injected blastomere, as judged from the often unilateral distribution of control *lacZ* RNA, as detected with anti-β-gal antibody (Promega, 1:500) after ISH. Embryos were fixed prior to ISH and antibody staining.

##### 4.5. Bead implantations, inhibitor treatment, morpholino injections

Bead implantations at shield stage and inhibitor treatments were done as described (Mohammadi et al., 1997; Reifers et al., 2000a). SU5402 inhibitor (Calbiochem) treatments were done at a final concentration of 16 µM before 24 hpf, or at 8 µM after 24 hpf, diluted into embryo medium from an 8 mM stock in dimethyl sulfoxide (DMSO); control treatments with DMSO dilution without inhibitor had no effect (not shown). Morpholino injections for *Mo-fgf8* were done as described in Araki and Brand (2001), for *Mo-fgf3* in Raible and Brand (2001); injections with four-base pair-mismatched (MM) control Mo's had no effect.

*Mo-fgf8*: GAGTCTCATGTTTATAGCCTCAGTA;  
*Mo-fgf8-MM*: GAGTCTGATCTTTTATAGCCACAGTA;  
*Mo-fgf3*: CAGTAACAACAAGAGCAGAATTATA;  
*Mo-fgf3-MM*: CACTAACAAGAAGACCACAATTATA.

In selected cases, the results were confirmed using a second *Mo-fgf3* (Phillips et al., 2001): CATTGTGGCATGGCGG-GATGTCCGC.

#### 4.6. Cell transplantations

Fertilized wild-type eggs, to be used as donors, were fluorescently labelled by injection of 7.5% tetramethylrhodamine and biotin, lysine fixable dextran (mini-ruby), 10.000 MW (Molecular Probes D-3312) in 0.25 M KCL. They were raised together with an unlabelled *ace* lay (to be used as hosts) to the shield stage. Cells from the wild-type donors embryos were then transplanted into the hosts. Host embryos were raised until the 10–12 somites stage and fixed overnight in 4% paraformaldehyde and a whole-mount RNA in situ hybridization to *pax2.1* was performed. The biotin lineage tracer in the transplanted cells was then detected in the host embryos using the ABC kit (Vector Labs). The host embryos were mounted in 70% glycerol for observation. For photography, embryos were dissected using electrolytically sharpened tungsten needles.

#### 4.7. Anti-phospho histone H3 staining

After ISH, embryos were washed 3 × 5 min in PBS + 0.1% Tween 20 (PBSTw) and blocked with 10% normal goat serum (NGS) in PBS + 0.8% Triton X-100 (PBSTx) for at least 1 h at room temperature. They were then incubated overnight at 4°C in the anti-phospho histone H3 primary antibody (rabbit polyclonal IgG; Upstate Biotechnology; 1:300 in 1% NGS-PBSTx) on a shaker. Embryos were washed 2 × 5 min and then 4 × 30 min in PBSTw. The endogenous peroxidases were blocked by washing 5 min in 50% MeOH/PBS, 5 min in 100% MeOH, 10 min in 0.30% H<sub>2</sub>O<sub>2</sub>/MeOH, 5 min in 50% MeOH/PBS and 5 min in PBS. Then, embryos were incubated overnight with the secondary antibodies (anti-rabbit IgG peroxidase conjugated, Sigma #A-6154; 1:200 in 1% NGS-PBSTx) on a shaker. Embryos were washed 2 × 5 and 4 × 30 min in PBSTw and 5 min in Tris 0.1 M pH 7.4. Embryos were then incubated with DAB peroxidase substrate (sigma, #D-4293). The color reaction was stopped by washing with PBSTw several times. The embryos were fixed 30 min in 4% PFA at room temperature, washed 2 × 5 min in PBSTw and cleared in 70% glycerol/PBSTw.

#### 4.8. Acridine orange (AO)

AO was applied to dechorionated embryos in E3 medium at a final concentration of 2 µg/ml for between 1 and 3 h. Excess AO was washed off by rinsing several times in E3 after this period. Fluorescence was monitored microscopically with FITC filter set (Hoechst).

## Acknowledgements

We thank the past and present members of the Brand laboratory for stimulating discussions and advice, in particular Frank Reifers and Alexander Picker. We furthermore thank Catherine Haddon for many a lobster, and her, Tanya Whitfield and Julian Lewis for stimulating discussions about ear development, and Tanya Whitfield for insightful comments on the manuscript. We also thank many zebrafish researchers, particularly Christine and Bernard Thisse and M. Kobayashi for kindly providing probes employed in this study, and Muriel Rhinn and Anukampa Barth for providing *mzoep* embryos. This work was supported by grants from the Deutsche Forschungsgemeinschaft, the EU (QLG3-CT-2001-02310), and the Max-Planck-Society.

## References

- Adamska, M., Legér, S., Brand, M., Hadrys, T., Bober, E., 2000. Expression of a new zebrafish inner ear and lateral line specific gene, *Nkx5-1*, is significantly reduced in the ears of *Fgf8* mutant, *ace*. *Mech. Dev.* 97, 161–165.
- Adamska, M., Herbrand, H., Adamski, M., Kruger, M., Braun, T., Bober, E., 2001. FGFs control the patterning of the inner ear but are not able to induce the full ear program. *Mech. Dev.* 109, 303–313.
- Akimenko, M.A., Ekker, M., Wegner, J., Lin, W., Westerfield, M., 1994. Combinatorial expression of three zebrafish genes related to distal-less: part of a homeobox gene code for the head. *J. Neurosci.* 14, 3475–3486.
- Araki, I., Brand, M., 2001. Antisense-morpholino-induced knockdown of *fgf8* phenocopies the *acerebellar* (*ace*) phenotype. *Genesis* 30, 157–159.
- Baker, C.V.H., Bronner-Fraser, M., 2001. Vertebrate cranial placodes. I. Embryonic induction. *Dev. Biol.* 232, 1–61.
- Brand, M., Heisenberg, C.-P., Jiang, Y.-J., Beuchle, D., Lun, K., van Eeden, F.J.M., Furutani-Seiki, M., Granato, M., Haffter, P., Hammerschmidt, M., Kane, D.A., Kelsh, R.N., Mullins, M.C., Odenthal, J., Nüsslein-Volhard, C., 1996. Mutations in zebrafish genes affecting the formation of the boundary between midbrain and hindbrain. *Development* 123, 179–190.
- Brand, M., Granato, M., Nüsslein-Volhard, C., 2002. Keeping and raising zebrafish. In: Nüsslein-Volhard, C., Dahm, R. (Eds.). *Zebrafish: A Practical Approach*, Oxford University Press, Oxford.
- Burgess, S., Reim, G., Chen, W., Hopkins, N., Brand, M., 2002. The zebrafish *spiel-ohne-grenzen* (*spg*) gene encodes the POU homeodomain protein Pou2 related to mammalian Oct4 and is essential for formation of the midbrain-hindbrain territory and early morphogenesis. *Development* 129, 905–916.
- Chambers, D., Mason, I., 2000. Expression of *sprouty2* during early development of the chick embryo is coincident with known sites of FGF signalling. *Mech. Dev.* 91, 361–364.
- Chisaka, O., Musci, T.S., Capecchi, M.R., 1992. Developmental defects of the ear, cranial nerves and hindbrain resulting from targeted disruption of the mouse homeobox gene *Hox-1.6* [see comments]. *Nature* 355, 516–520.
- Cordes, S.P., Barsh, G.S., 1994. The mouse segmentation gene *kr* encodes a novel basic domain-leucine zipper transcription factor. *Cell* 79, 1025–1034.
- Deol, M.S., 1964. The abnormalities of the inner ear in *kreisler* mice. *J. Embryol. Expt. Morphol.* 12, 475–490.
- Deol, M.S., 1966. Influence of the neural tube on the differentiation of the inner ear in the mammalian embryo. *Nature* 209, 219–220.
- Dolle, P., Lufkin, T., Krumlauf, R., Mark, M., Duboule, D., Chambon, P., 1993. Local alterations of *Krox-20* and *Hox* gene expression in the

- hindbrain suggest lack of rhombomeres 4 and 5 in homozygote null *Hoxa-1* (*Hox-1.6*) mutant embryos. *Proc. Natl. Acad. Sci. USA* 90, 7666–7670.
- Ekker, M., Akimenko, M.A., Bremiller, R., Westerfield, M., 1992. Regional expression of three homeobox transcripts in the inner ear of zebrafish embryos. *Neuron* 9, 27–35.
- Epstein, D.J., Vekemans, M., Gros, P., 1991. *Splotch* (*Sp2H*), a mutation affecting development of the mouse neural tube, shows a deletion within the paired homeodomain of *Pax-3*. *Cell* 67, 767–774.
- Fekete, D.M., 1996. Cell fate specification in the inner ear. *Curr. Opin. Neurobiol.* 6, 533–541.
- Fritsch, B., Barald, K.F., Lomax, M.I., 1998. Early embryology of the vertebrate ear. In: Rubel, R.W., Popper, A.N., Fay, R.R. (Eds.). *Development of the Auditory System*, 9. Springer, New York, pp. 80–145.
- Frohman, M.A., Martin, G.R., Cordes, S.P., Halamek, L.P., Barsh, G.S., 1993. Altered rhombomere-specific gene expression and hyoid bone differentiation in the mouse segmentation mutant, *kreisler* (*kr*). *Development* 117, 925–936.
- Fürthauer, M., Thisse, C., Thisse, B., 1997. A role for *Fgf-8* in the dorsoventral patterning of the zebrafish gastrula. *Development* 124, 4253–4264.
- Fürthauer, M., Reifers, F., Brand, M., Thisse, B., Thisse, C., 2001. *sprouty4* acts in vivo as a feedback-induced antagonist of *Fgf* signaling in zebrafish. *Development* 128, 2175–2186.
- Gallagher, B.C., Henry, J.J., Grainger, R.M., 1996. Inductive processes leading to inner ear formation during *Xenopus* development. *Dev. Biol.* 175, 95–107.
- Gegenbaur, C., 1898. Vergleichende Anatomie der Wirbeltiere mit Berücksichtigung der Wirbellosen. Wilhelm Engelmann, Leipzig, I, 874–910.
- Gritsman, K., Zhang, J., Cheng, S., Heckscher, E., Talbot, W.S., Schier, A.F., 1999. The EGF-CFC protein one-eyed pinhead is essential for nodal signaling. *Cell* 97, 121–132.
- Groves, A.K., Bronner-Fraser, M., 2000. Competence, specification and commitment in otic placode induction. *Development* 127, 3489–3499.
- Haddon, C., Lewis, J., 1996. Early ear development in the embryo of the zebrafish, *Danio rerio*. *J. Comp. Neurol.* 365, 113–128.
- Harrison, R.G., 1935. Factors concerned in the development of the ear in *Amblystoma punctatum*. *Anat. Rec.* 64, 38–39.
- Harrison, R.G., 1945. Relations of symmetry in the developing embryo. *Trans. Conn. Acad. Arts Sci.* 36, 277–330.
- Jacobson, A.G., 1963a. The determination and positioning of the nose, lens and ear. I. Interactions within the ectoderm, and between the ectoderm and underlying tissues. *J. Exp. Zool.* 154, 273–283.
- Jacobson, A.G., 1966. Inductive processes in embryonic development. *Science*, 152, 25–34.
- Jørgensen, J.M., 1989. Evolution of octavolateralis sensory cells. In: Coombs, S., Görner, P., Münz, H. (Eds.). *The Mechanosensory Lateral Line: Neurobiology and Evolution*, Springer-Verlag, New York, pp. 187–216.
- Kiefer, P., Strahle, U., Dickson, C., 1996. The zebrafish *Fgf-3* gene: cDNA sequence, transcript structure and genomic organization. *Gene* 168, 211–215.
- Kimmel, C.B., Ballard, W.W., Kimmel, S.R., Ullmann, B., Schilling, T.F., 1995. Stages of embryonic development of the zebrafish. *Dev. Dyn.* 203, 253–310.
- Kinoshita, N., Minshull, J., Kirschner, M.W., 1995. The identification of two novel ligands of the FGF receptor by a yeast screening method and their activity in *Xenopus* development. *Cell* 83, 621–630.
- Kobayashi, M., 2000. Six family genes as key factors in the sensory organ formation. *Tanpakushitsu Kakusan Koso* 45, 2775–2781.
- Korz, V., Sleptsova, I., Liao, J., He, J., Gong, Z., 1998. Expression of the zebrafish bHLH genes *ngn1* and *nrd* defines distinct stages of neural differentiation. *Dev. Dyn.* 213, 92–104.
- Krauss, S., Johansen, T., Korzh, V., Fjose, A., 1991. Expression of the zebrafish paired box gene *pax[*zf*-b]* during early neurogenesis. *Development* 113, 1193–1206.
- Kuwada, J.Y., Bernhardt, R.R., Chitnis, A.B., 1990. Pathfinding by identified growth cones in the spinal cord of zebrafish embryos. *J. Neurosci.* 10, 1299–1308.
- Kozłowski, D.J., Murakami, T., Ho, R.K., Weinberg, E.S., 1997. Regional cell movement and tissue patterning in the zebrafish embryo revealed by fate mapping with caged fluorescein. *Biochem. Cell Biol.* 75, 551–562.
- Ladher, R.K., Anakwe, K.U., Gurney, A.L., Schoenwolf, G.C., Francis-West, P.H., 2000. Identification of synergistic signals initiating inner ear development. *Science* 290, 1965–1967.
- Li, Y., Allende, M.L., Finkelstein, R., Weinberg, E.S., 1994. Expression of two zebrafish orthodenticle-related genes in the embryonic brain. *Mech. Dev.* 48, 229–244.
- Lombardo, A., Slack, J.M., 1998. Postgastrulation effects of fibroblast growth factor on *Xenopus* development. *Dev. Dyn.* 212, 75–85.
- Lombardo, A., Isaacs, H.V., Slack, J.M., 1998. Expression and functions of FGF-3 in *Xenopus* development. *Int. J. Dev. Biol.* 42, 1101–1107.
- Lufkin, T., Dierich, A., LeMeur, M., Mark, M., Chambon, P., 1991. Disruption of the *Hox-1.6* homeobox gene results in defects in a region corresponding to its rostral domain of expression. *Cell* 66, 1105–1119.
- Mahmood, R., Kiefer, P., Guthrie, S., Dickson, C., Mason, I., 1995. Multiple roles for FGF-3 during cranial neural development in the chicken. *Development* 121, 1399–1410.
- Malicki, J., Schier, A.F., Solnica-Krezel, L., Stemple, D.L., Neuhauss, S.C., Stainier, D.Y., Abdelilah, S., Rangini, Z., Zwartkruis, F., Driever, W., 1996. Mutations affecting development of the zebrafish ear. *Development* 123, 275–283.
- Mansour, S.L., Goddard, J.M., Capecchi, M.R., 1993. Mice homozygous for a targeted disruption of the proto-oncogene *int-2* have developmental defects in the tail and inner ear. *Development* 117, 13–28.
- Mark, M., Lufkin, T., Vonesch, J.L., Ruberte, E., Olivo, J.C., Dolle, P., Gorry, P., Lumsden, A., Chambon, P., 1993. Two rhombomeres are altered in *Hoxa-1* mutant mice. *Development* 119, 319–338.
- Maroon, H., Walshe, J., Mahmood, R., Kiefer, P., Dickson, C., Mason, I., 2002. *Fgf3* and *Fgf8* are required together for formation of the otic placode and vesicle. *Development* 129, 2099–2108.
- Maves, L., Jackman, W., Kimmel, C.B., 2002. FGF3 and FGF8 mediate a rhombomere 4 signaling activity in the zebrafish hindbrain. *Development* 129, 3825–3837.
- McKay, I.J., Muchamore, I., Krumlauf, R., Maden, M., Lumsden, A., Lewis, J., 1994. The *kreisler* mouse: a hindbrain segmentation mutant that lacks two rhombomeres. *Development* 120, 2199–2211.
- McKay, I.J., Lewis, J., Lumsden, A., 1996. The role of FGF-3 in early inner ear development: an analysis in normal and *kreisler* mutant mice. *Dev. Biol.* 174, 370–378.
- Mendonsa, E.S., Riley, B.B., 1999. Genetic analysis of tissue interactions required for otic placode induction in the zebrafish. *Dev. Biol.* 206, 100–112.
- Moens, C.B., Yan, Y.L., Appel, B., Force, A.G., Kimmel, C.B., 1996. *valentino*: a zebrafish gene required for normal hindbrain segmentation. *Development* 122, 3981–3990.
- Moens, C.B., Cordes, S.P., Giorgianni, M.W., Barsh, G.S., Kimmel, C.B., 1998. Equivalence in the genetic control of hindbrain segmentation in fish and mouse. *Development* 125, 381–391.
- Mohammadi, M., McMahon, G., Sun, L., Tang, C., Hirth, P., Yeh, B.K., Hubbard, S.R., Schlessinger, J., 1997. Structures of the tyrosine kinase domain of fibroblast growth factor receptor in complex with inhibitors. *Science* 276, 955–960.
- Morsli, H., Tuorto, F., Choo, D., Postiglione, M.P., Simeone, A., Wu, D.K., 1999. *Otx1* and *Otx2* activities are required for the normal development of the mouse inner ear. *Development* 126, 2335–2343.
- Münchberg, S.R., Ober, E.A., Steinbeisser, H., 1999. Expression of the *Ets* transcription factors *erm* and *pea3* in early zebrafish development. *Mech. Dev.* 88, 233–236.
- Nasevicius, A., Ekker, S.C., 2000. Effective targeted gene ‘knockdown’ in zebrafish. *Nat. Genet.* 26, 216–220.
- Nicolson, T., Rusch, A., Friedrich, R.W., Granato, M., Ruppertsberg, J.P., Nusslein-Volhard, C., 1998. Genetic analysis of vertebrate sensory hair

- cell mechanosensation: the zebrafish circler mutants. *Neuron* 20, 271–283.
- Northcutt, R.G., 1986. Evolution of the octavolateralis system: evaluation and heuristic value of phylogenetic hypotheses. In: Rubel, R.W., Van de Water, T.R., Rubel, E.W. (Eds.). *The Biology of Change in Otolaryngology*, Elsevier, New York, pp. 3–14.
- Pfeffer, P.L., Gerster, T., Lun, K., Brand, M., Busslinger, M., 1998. Characterization of three novel members of the zebrafish *Pax2/5/8* family: dependency of *Pax5* and *Pax8* expression on the *Pax2.1(noi)* function. *Development* 125, 3063–3074.
- Phillips, B.T., Bolding, K., Riley, B.B., 2001. Zebrafish *fgf3* and *fgf8* encode redundant functions required for otic placode induction. *Dev. Biol.* 235, 351–365.
- Picker, A., Brennan, C., Reifers, F., Clarke, J.D., Holder, N., Brand, M., 1999. Requirement for the zebrafish mid-hindbrain boundary in midbrain polarisation, mapping and confinement of the retinotectal projection. *Development* 126, 2967–2978.
- Picker, A., Scholpp, S., Böhli, H., Takeda, H., Brand, M., 2002. A novel positive transcriptional feedback loop in midbrain-hindbrain boundary development is revealed through analysis of the zebrafish *pax2.1* promoter in transgenic lines. *Development* 129, 3227–3239.
- Platt, C., Popper, A.N., Fay, R.R., 1989. The ear as a part of the octavolateralis system. In: Coombs, S. (Ed.). *The Mechanosensory Lateral Line*, Springer, Berlin, Heidelberg, New York, pp. 633–651.
- Raible, F., Brand, M., 2001. Tight transcriptional control of the ETS domain factors *Erm* and *Pea3* by FGF signaling during early zebrafish nervous system development. *Mech. Dev.* 107, 105–117.
- Reifers, F., Böhli, H., Walsh, E.C., Crossley, P.H., Stainier, D.Y.R., Brand, M., 1998. *Fgf8* is mutated in zebrafish *acerebellar* mutants and is required for maintenance of midbrain-hindbrain boundary development and somitogenesis. *Development* 125, 2381–2395.
- Reifers, F., Adams, J., Mason, I., Schulte-Merker, S., Brand, M., 2000a. Overlapping and distinct functions provided by *fgf17*, a new zebrafish member of the *Fgf8/17/18* subgroup of Fgfs. *Mech. Dev.* 99, 39–49.
- Reifers, F., Walsh, E.C., Léger, S., Stainier, D.Y.R., Brand, M., 2000b. Induction and differentiation of the zebrafish heart requires fibroblast growth factor 8 (*Fgf8/acerebellar*). *Development* 127, 225–235.
- Reim, G., Brand, M., 2002. *spiel-ohne-grenzen/pou2* mediates regional competence to respond to *Fgf8* during zebrafish early neural development. *Development* 129, 917–933.
- Represa, J., Leon, Y., Miner, C., Giraldez, F., 1991. The int-2 proto-oncogene is responsible for induction of the inner ear. *Nature* 353, 561–563.
- Riley, B.B., Grunwald, D.J., 1996. A mutation in zebrafish affecting a localized cellular function required for normal ear development. *Dev. Biol.* 179, 427–435.
- Riley, B.B., Zhu, C., Janetopoulos, C., Aufderheide, K.J., 1997. A critical period of ear development controlled by distinct populations of ciliated cells in the zebrafish. *Dev. Biol.* 191, 191–201.
- Rupp, R.A.W., Snider, L., Weintraub, H., 1994. *Xenopus* embryos regulate the nuclear localization of XMyoD. *Genes Dev.* 8, 1311–1323.
- Sahly, I., Andermann, P., Petit, C., 1999. The zebrafish *eya1* gene and its expression pattern during embryogenesis. *Dev. Genes Evol.* 209, 399–410.
- Schier, A.F., Shen, M.M., 2000. Nodal signalling in vertebrate development. *Nature* 403, 385–389.
- Sechrist, J., Scherson, T., Bronner-Fraser, M., 1994. Rhombomere rotation reveals that multiple mechanisms contribute to the segmental pattern of hindbrain neural crest migration. *Development* 120, 1777–1790.
- Servetnick, M., Grainger, R.M., 1991. Changes in neural and lens competence in *Xenopus* ectoderm: evidence for an autonomous developmental timer. *Development* 112, 177–188.
- Shamim, H., Mason, I., 1999. Expression of *Fgf4* during early development of the chick embryo. *Mech. Dev.* 85, 189–192.
- Shanmugalingam, S., Houart, C., Picker, A., Reifers, F., MacDonald, R., Barth, A.K., Brand, M., Wilson, S.W., 2000. *Ace/Fgf8* is required for forebrain commissure formation and patterning of the telencephalon. *Development* 127, 2549–2561.
- Sharman, A.C., Brand, M., 1998. Evolution and homology of the nervous system: cross-phylum rescues of *otd/Otx* genes. *Trends Genet.* 14, 211–214.
- Slack, J.M., 1995. Developmental biology. Growth factor lends a hand. *Nature* 374, 217–218.
- Steel, K.P., 1995. Inherited hearing defects in mice. *Annu. Rev. Genet.* 29, 675–701.
- Stone, L.S., 1931. Induction of the ear by the medulla and its relation to experiments on the lateralis system in amphibia. *Science* 74, 577.
- Tannahill, D., Isaacs, H.V., Close, M.J., Peters, G., Slack, J.M., 1992. Developmental expression of the *Xenopus int-2* (FGF-3) gene: activation by mesodermal and neural induction. *Development* 115, 695–702.
- Thisse, C., Thisse, B., Postlethwait, J.H., 1995. Expression of *snail2*, a second member of the zebrafish *snail* family, in cephalic mesendoderm and presumptive neural crest of wild-type and *spadetail* mutant embryos. *Dev. Biol.* 172, 86–99.
- Thisse, C., Thisse, B., Halpern, M.E., Postlethwait, J.H., 1994. Goosecoid expression in neurectoderm and mesendoderm is disrupted in zebrafish *cyclops* gastrulas. *Dev. Biol.* 164, 420–429.
- Torres, M., Giraldez, F., 1998. The development of the vertebrate inner ear. *Mech. Dev.* 71, 5–21.
- Van de Water, T.R., Conley, X., 1982. Neural inductive message to the developing mammalian inner ear: contact mediated versus extracellular matrix interaction. *Anat. Rec.*, 195A.
- Van de Water, T.R., Represa, J., 1991. Tissue interactions and growth factors that control development of the inner ear. Neural tube-otic anlage interaction. *Ann. NY Acad. Sci.*, 630, 116–128.
- Vendrell, V., Carnicero, E., Giraldez, F., Alonso, M.T., Schimmang, T., 2000. Induction of inner ear fate by FGF3. *Development* 127, 2011–2019.
- Waddington, C.H., 1937. The determination of the auditory placode in the chick. *J. Exp. Biol.* 14, 232–239.
- Westerfield, M., 1994. *The Zebrafish Book*, 2.1 Edition. University of Oregon Press, Oregon.
- Whitfield, T.T., Riley, B.B., Chiang, M.Y., Phillips, B., 2002. Development of the zebrafish inner ear. *Dev. Dyn.* 223, 427–458.
- Whitfield, T., Granato, M., van Eeden, F.J.M., Schach, U., Brand, M., Furutani-Seiki, M., Haffter, P., Hammerschmidt, M., Heisenberg, C.-P., Jiang, Y.-J., Kane, D.A., Kelsh, R.N., Mullins, M.C., Odenthal, J., Nüsslein-Volhard, C., 1996. Mutations affecting development of the zebrafish inner ear and lateral line. *Development* 123, 241–254.
- Whitlock, K.E., Westerfield, M., 2000. The olfactory placodes of the zebrafish form by convergence of cellular fields at the edge of the neural plate. *Development* 127, 3645–3653.
- Wilkinson, D.G., Peters, G., Dickson, C., McMahon, A.P., 1988. Expression of the FGF-related proto-oncogene *int-2* during gastrulation and neurulation in the mouse. *EMBO J.* 7, 691–695.
- Woo, K., Fraser, S.E., 1998. Specification of the hindbrain fate in the zebrafish. *Dev. Biol.* 197, 283–296.
- Yntema, C.L., 1950. An analysis of induction of the ear from foreign ectoderm in the salamander embryo. *J. Exp. Zool.* 113, 211–240.
- Yntema, C.L., 1955. Ear and nose. *Analysis of Development*, Saunders, Philadelphia/London, pp. 415–428.
- Zwilling, E., 1941. The determination of the otic vesicle in *Rana pipiens*. *J. Exp. Zool.* 86, 333–342.